Investigation of Gauge-Gravity duality via 2D $\mathcal{N} = (8, 8)$ Super-Yang-Mills lattice simulations

(2D $\mathcal{N}$=(8,8) Super-Yang-Mills 理論の格子シミュレーションによるゲージ重力双対性の研究)

Eric Giguère

Hokkaido University
Graduate school of science
Department of physics
Theoretical particle physics research group

August 12, 2015

Abstract

We study the gauge-gravity duality between supersymmetric $\mathcal{N} = (8, 8)$ super Yang-Mills theory in two dimensions and the supergravity solution of D1-brane in IIB string theory. Through lattice simulations, we estimate physical quantities of the gauge theory and compare them with the dual quantity from black string thermodynamics. In this study, we use Sugino's formulation for $\mathcal{N} = (8, 8)$ super Yang-Mills in two dimensions. It is the first simulations performed using this formulation so we first test its validity. We confirm that the lattice artifacts of the model disappear in the continuum limit, then we observe restoration of the full supersymmetry using the supersymmetric Ward-Takahashi identity. We also verify the simulation results using perturbative calculations in the low coupling region. Lastly we compare the thermodynamic quantity $E - PV$ obtained from the lattice simulations of super Yang-Mills theory with the calculation done in the gravity side. We find a good agreement at low temperature where the duality is expected to hold.

ACKNOWLEDGEMENTS

I am grateful to Kadoh Daisuke for guiding me and teaching me during this research, without his collaboration this thesis would not have been possible. I am also sincerely grateful for my supervisors, Kawamoto Noboru for introducing me to lattice theory and teaching me, and Nakayama Ryuichi for feedback and support.

I would like to thank everyone in the particle physics department in Hokkaido University for their warm welcome.

I am grateful for the Scholarship from the Monbukagakusho, without which, I would not be able to study and to experience Japan so fully.

I would also like to thank the facilities that were used for the computations: the RIKEN Integrated Cluster of Clusters (RICC) facility, RIKEN's K computer, KEK supercomputer and SR16000 at YITP in Kyoto University.

Lastly I would like to thank my family for their support and encouragement.

Contents

Overview

In physics, connections between different theories often take surprising forms. Some of such connections form the core of our present understanding of the world, such as the particle/wave duality of quantum physics. Some other connect seemingly unrelated sciences, such as the electrodynamics being applied to economic models[1]. But in present theoretical physics, the collection of gauge-gravity dualities probably attracts the most attention due to the unexpected connections.

These gauge-gravity duality started with the discovery of the correspondence between Anti-de Sitter space and Conformal field theory proposed by Malcadena[2]. Through the study of D-brane in string theory, it was suggested that string IIB on $AdS_5 \times S_5$ is equivalent to $\mathcal{N} = 4$ supersymmetric Yang-Mills theory in four dimensions. This first AdS/CFT duality was quickly followed by others, such as the correspondence between $AdS_4 \times S_7$ and ABJM superconformal field theory[3]. It was also understood that the duality could be generalized to non-conformal case. It was argued that p-brane solution of supergravity is dual to the maximally supersymmetric super Yang-Mills(SYM) in $(p+1)$ dimensions [4].

This last series of dualities, the black p-brane/$D = (p + 1)$ SYM, is particularly interesting from the gauge theory point of view. The means to study the large coupling region of the SYM has been greatly improved in the last decade. Developments in supersymmetric lattice model make it possible to test the duality conjecture with numerical simulation.

In section 1, we first present a simple argument to explain the dualities. This is followed by a review of the confirmations of the duality using numerical methods. Lastly we examine the development of lattice supersymmetry.

The thesis is organized as follows. In section 2, we explain the lattice formulation of the $\mathcal{N} = 16$, $D = 2$ SYM, with it's diverse concerns. In section 3, we present compelling results of simulations that show the validity of the lattice model. This include verifying the disappearance of the lattice artifact in the continuum limit and the restoration of the full supersymmetry. This is followed with comparison with calculation from perturbation theory. In section 4, the dual theory in the gravity side is introduced. After preparing a physical quantity that can be obtained from both side of the duality we make the explicit comparison of the theories in section 4.3.

1 Introduction

1.1 The ADS/CFT duality

The duality conjecture was discovered in the study of superstring theory. String theory started as a tool to understand QCD. Quarks would be connected by strings, whose energies depend on their length, causing confinement. But it was soon realized that instead of QCD, a gravity theory naturally emerged: propagating closed strings behaved like gravitons. The string, being a 1+1 dimensional object instead of a point object, is free of divergence, the extended nature of the string would serve as a natural regularization. Thus string theory became a popular candidate for quantum gravity. But a gravity theory should couple with matter and simple strings are bosonic. However, with the

insertion of supersymmetry, the fermions could also be inserted in the theory. Another interesting fact of string theory is that the number of dimensions is not imposed, but derived. Superstring need a ten dimensional spacetime in order to be mathematically consistent. The extra dimensions are usually compactified and depending on the exact compactification, a wide range of elementary particles can emerge.

Around 1990, it was recognized that type II string theory could not be made only of string. In addiction to the 1+1 dimensional string, the theory needed p+1 dimensional objects called Dp-brane[5]. These branes served as an anchor for the open strings to attach themselves to. The branes can interact by emitting and receiving closed strings, which propagate freely in the whole space. Branes can also be connected by open strings.

It was realized that, at large string coupling, Dp-branes are equivalent to Extremal Black p-brane in supergravity [6][7]. The equivalence was established on the realization that both are p-dimensional object with the same R-R charge. The D-brane and black p-brane are two limits of the same object. By varying the string coupling adiabatically, it is possible to connect both description[8]. From those two approach, the AdS/CFT duality was constructed.

When studying the Dp-branes with a perturbation approach, we consider N coinciding D3-brane in a 10 dimensional spacetime. The branes are connected to each by open string and interact with the closed string propagating in the bulk (the spacetime around the brane). The model is studied using worldsheet expansion, each worldsheet is responsible for a gN contribution, g being the string coupling constant. Thus this model can be understood with perturbation theory when gN is small. In the low energy limit, string exited states disappear and the string length gets shorter ($\alpha' \to 0$). The remaining open string behave like gauge particle on the 3+1 dimensional brane. They form the $\mathcal{N} = 4$, $D = 4$, $U(N)$ SYM. The closed string mode in the bulk decouple from the brane's physics at low energy and can be ignored.

In the black 3-brane side, the open strings are hidden while closed string still fill the bulk. The physics of the black brane is contained in its black-hole nature: it has an horizon, an entropy and deform the spacetime. The metric is given by

$$ds^2 = H^{-1/2}(r)(-dt^2 + dx_\parallel^2) + H^{1/2}(r)dx_\perp^2, \qquad (1)$$
$$H = 1 + \frac{L^4}{r^4} \qquad L^4 = 4\pi g N \alpha'^2$$

where the $x_\parallel$ are dimensions on the brane and $x_\perp$ are the dimensions of the bulk. This theory is well understood when the typical scale of the space is greater than the string scale ($L^2 \gg \alpha'$) and quantum effect can be ignored. Therefore this model is studied at large gN which corresponds to the classical limit. Looking at the low energy limit, we have massless closed string in the bulk and the $r \to 0$ physics. Here again, the close strings in the bulk decouple from the brane and can be ignored. Close to the brane ($r \to 0$), the function $H^{-1/2}(r)$ goes to zero suppressing the energies. In this limit, the spacetime take a Anti-de Sitter form

$$ds^2 = \frac{r^2}{L^2}(-dt^2 + dx_\parallel^2) + \frac{L^2}{r^2}dr^2 + L^2 d\Omega_5. \qquad (2)$$

The three dimensions on the brane with the time t and the radius r form the AdS_5 space and the remaining five dimensions form a five dimensional sphere S_5 of radius L.

Connecting the parts together, we have Maldacenna's ADS/CFT conjecture. The low energy limit of D3-brane is the $\mathcal{N} = 4$, $D = 4$, $U(N)$ SYM theory. However the D3-brane can be seen as black 3-brane which low energy limit is a supergravity theory with a $AdS_5 \times S_5$ spacetime. Therefore, the SYM theory should be dual to the supergravity theory. This should be true as long as taking the low energy limit commutes with the transition from both point of view.

The validity of the dualities is strongly supported. Both side have the same symmetries, and a matching spectra of supersymmetric states[9]. Both side have the important conformal symmetry. With this symmetry, some calculations can be done at any coupling, including the strongly coupled gauge theory which cannot be treated using perturbation theory, allowing many verifications. Also, based on the conformal theory, a dictionary connecting physical quantities on both side of the duality was created [10][11].

The AdS/CFT conjecture connects a gravity theory in its weak coupling regime with a gauge theory with strong coupling. This opens the door to studing strongly coupled gauge theories on the easier gravity side[12], [13]. Moreover, it could potentially allow the solving of quantum gravity model using understood gauge model. The understanding of some questions, such as the black hole information loss paradox, could be improved by using the duality[14].

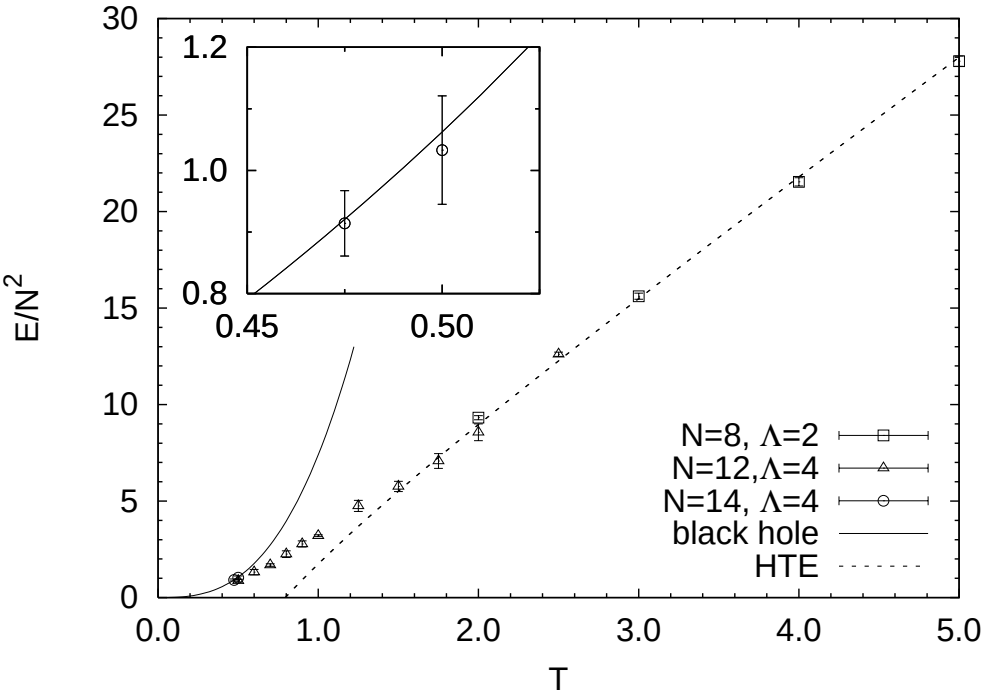

Figure 1: Internal energy of $\mathcal{N} = 16$ SYM in one dimension computed using the matrix model obtained by Nishimura et al.[15]. The lines are the theoretical predictions from black 0-brane solution (full line) and high temperature expansion (dashed line). The gauge-gravity conjecture indicate that at low temperature, where the supergravity calculation can be trusted, the results from the gauge theory should be consistent with the gravity calculation. At low temperature, the simulation results did match the gravity curve.

1.2 Gauge gravity duality in lower dimension

From the study of D3-brane, the AdS/CFT duality conjecture came out, which is strongly supported. However, this duality give a hint of a bigger duality; we can do the demonstration using a general Dp-brane instead of a D3-brane. In the gauge theory side, with a similar line of reasoning, we obtain the $D = p + 1$ maximally supersymmetric SYM. In the supergravity side, we get the $r \to 0$ limit of Black p-brane. The resulting duality between gauge and gravity was first suggested by Maldacena et al. in 1998. When $p \neq 3$, the gauge field theory is not conformal and the resulting spacetime is not anti-de Sitter. The conformal symmetry is replaced by another set of symmetries that are equivalent both side of the duality. However without conformal symmetry, the duality conjecture is a lot harder to verify, exact calculations being very complex, if not impossible. Therefore a lot less evidence has been accumulated to back it up. For the low dimensions case, the few verifications that were obtained used numerical simulations.

The first successful test was performed by Nishimura et al.[15] in 2007. Using a matrix model with a simple ultraviolet cut-off as regularization, they compared the energy of the $N = 16$ SYM in one dimension at finite temperature with the internal energy of the dual black-hole. They observed a good agreement between gauge theory simulations and supergravity calculation, (figure 1). Their study included the effect of string length (α' corrections) and string loop effect (finite N expansion). The weakness of their method is the use of matrix model which is only valid in 1D.

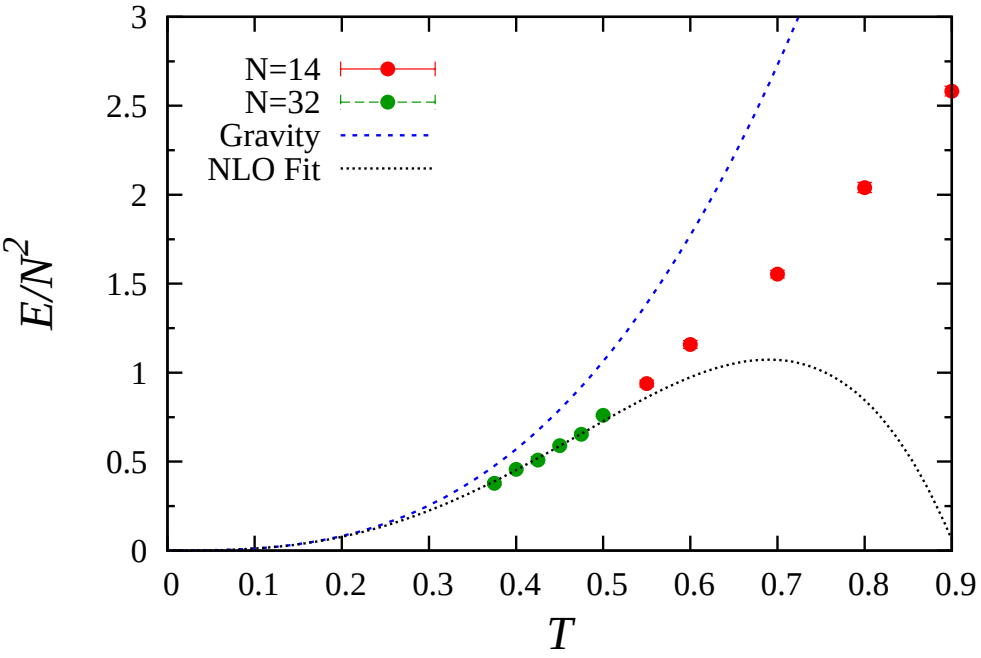

Figure 2: Internal energy of $\mathcal{N} = 16$ SYM in one dimension computed using Sugino's lattice model obtained by Kadoh and Kamata [16]. The blue 'Gravity' line is the theoretical prediction from black 0-brane solution at the leading order. The dashed curve is the next to leading order obtained with a fit. The fit is consistent with the expectations.

Following the success of Nishimura et al. came Kadoh and Kamata reproduction of the result using lattice theory. With lattice theory, attention is made to keep gauge symmetry and partial supersymmetry exact. Because of this extra difficulty the results came a few years after the matrix model resutl, in 2015[16]. They also were able to see agreement between the supergravity theory and $\mathcal{N} = 16$ SYM,(figure 2). The advantage of lattice theory is that it can be also be extended two dimensions with reasonable ease.

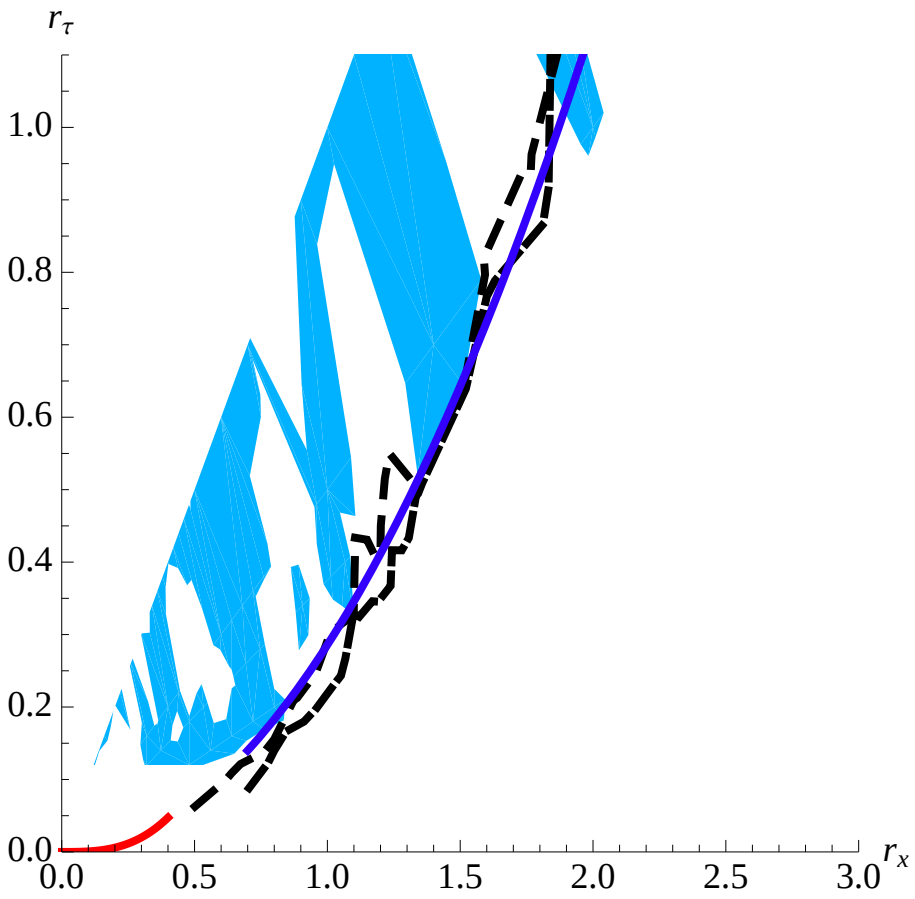

Figure 3: Boundary of the phase transition between the IIA and IIB string theory regime obtained by Catterall et al.[17] using lattice simulation of $\mathcal{N} = (8, 8)$, $D = 2$ SYM. The y unit is the unitless temporal direction volume and the x unit is the unitless spacial volume. The blue zone correspond to a black 0-brane regime or non null spatial Polyakov line $P_x \approx 1$, the other zone correspond to a black 1-brane phase, $P_x \approx 0$. The black lines are the measured locations of the phase transition, called Gregory-Laflamme phase transition, obtained using different group size $N = 3,\ 4$. The blue line is the numerical fit with the expected shape obtained supergravity $r_x^2 = cr_\tau$, with a fitted $c \approx 3.5$, well within the constraint from gravity $c > 2.29$.

Up to now, only indirect test of the duality were made for $\mathcal{N} = (8, 8)$, $D = 2$ SYM with D1-brane in IIB string theory. In 2010 Catterall, Joseph, Wiseman used lattice SYM simulations to observe a phase transition predicted in supergravity (figure 3)[17]. The Gregory-Laflamme phase transition is a phenomenon that occur in D1-brane.

When the length of the D1-brane is small compared to the theory coupling constant (temperature), the physics of the brane become to those of a D0-brane. In the gauge side, the phase transition can be observed by calculating the Polyakov line in the spacial direction, the D0-brane corresponds to $P_x \approx 1$ while the D1-brane corresponds to $P_x = 0$. Using simulation of two dimensional SYM, they were able to observe the phase transition conditions and found them in accordance with the prediction from the string model. This indirect test support the validity of the correspondence in two dimension. However the authors did not do any direct verification such as the comparisons of the energy both side of the duality. [1]

In the present study, we want to fill this gap by making a direct comparison between $\mathcal{N} = (8, 8)$, $D = 2$ SYM and extremal black 1-brane to obtain direct evidence of the duality.

1.3 Supersymmetry and lattice theory

Calculations in quantum fields theory are not trivial. Interactions between the different component of the model give rise to the dynamic and interesting physics. However, rarely such model can be exactly solved. Moreover, the theory contains divergences which must be regularized to obtain meaningful physical quantities. In a theory with low coupling constant, perturbation theory can be used to incorporate the physics of the interactions. With perturbation theory, the divergence can be regularized order by order using one of many known method, such as dimensional regularization. However, for theories with a strong coupling, this method cannot be applied since higher terms of the approximation do not become insignificant.

Lattice theory was developed to tackle these cases. The discretization of the space time introduced by the lattice serve as a regularization of the UV divergence of the system. Lattice theory also define the field theory with a finite number of degree of freedom, making the problem solvable at any coupling, providing that sufficient computing power is available. However going to the lattice break the Lorentz symmetry and infinitesimal translation symmetry which are only restored in the continuous limit. On the other hand, gauge symmetry and other internal symmetries are usually kept exact on the lattice. Lattice was first used to study QCD, explaining the confinement of quark[18]. It is also used to calculate the hadron spectrum and gives excellent agreement with experimental results.

While lattice is mainly used for QCD-like model, the increasing popularity of supersymmetry and the importance of understanding it in the non-perturbative regime created the need for a lattice formulation of supersymmetric model. This is not a simple matter as two problems arise when putting supersymmetry on the lattice: the presence of fermion doublers and the breaking of the Leibniz rule for the difference operator.

On the lattice, derivatives do not exist and are replaced by difference operator. This

[1] The lattice model used by Catterall et al. breaks supersymmetry on the lattice. This is probably the reason they were unable to find an agreement of the duality in 1D when they attempted a direct test[**?**], therefore went for an indirect test in 2D.

has the effect of changing the momentum of the fermion in the action to a sine form

$$S = \int \frac{\mathrm{d}p^d}{(2\pi)^d} i\bar{\Psi}(-p)p_\mu\gamma_\mu\Psi(p) \to \int_{-\pi}^{\pi} \frac{\mathrm{d}p^d}{(2\pi)^d} i\bar{\Psi}(-p)sin(p_\mu)\gamma_\mu\Psi(p) \tag{3}$$

Inside of the lattice Brillouin zone, there are 2 solutions, $p_\mu = 0$ and $p_\mu = \pi$, that correspond to on-shell fermions. Each modes survive in the continuum limit and posses a different chirality. Since the fermion described are massless particle, Lorentz transformation cannot change chirality, leading to the realization that these solutions correspond to different particles. Therefore, when trying to put one fermions on the lattice, it is doubled for each spacetime directions, resulting in 2^d particles. It was shown that the doublers cannot be removed without breaking some important property[19]:

- Locality
- Translation invariance
- Chirality
- Hermiticity of the fermion action

This is particularly problematic for supersymmetric models since the theory need the same number of fermions and bosons, therefore the extra degrees of freedom break the supersymmetry.

The other problem facing lattice supersymmetry is the breaking of Leibniz rule. The supersymmetry algebra contain derivative, however infinitesimal translations do not exist on the lattice. The problem arises when applying supertransformation to a lattice elements. The superalgebra is distributive

$$Q(\phi\psi) = Q(\phi)\psi \pm \phi Q(\psi), \tag{4}$$

where Q is the fermionic supercharge and ϕ and ψ are either bosonic or fermionic fields. However the difference operator is not distributive, for example in the symmetric difference operator case we have

$$\nabla(\phi(x)\psi(x)) = \nabla(\phi(x))\psi(x+a) + \phi(x-a)\nabla(\psi(x)), \tag{5}$$

where $\nabla(\phi(x)) = \phi(x+a) + \phi(x-a)$, with a being the lattice spacing. Because the superalgebra is connected to the derivative by $Q^2 = i\partial$, supersymmetry cannot be trivially constructed on the lattice. This also gave rise to a no-go theorem stating that it is impossible to have translation invariance, locality and Leibniz rule at the same time on the lattice[20].

From these no-go theorems, it is easy to see that simple lattice theory breaks supersymmetry. In recent years, many methods to manage these issues leaded to a multitude of lattice supersymmetric models[21], [22], [23], [24], [25], [26], [27], [28], [29], [30] . These models splits in three main approaches.

First, give up on supersymmetry at the lattice level and expect that, similarly to Lorentz symmetry, the supersymmetry is recovered in the continuous limit. These methods usually use fine-tuning of some parameters to obtain the desired continuum theory[31].

Secondly, there is the opposite approach of forcing full supersymmetry on the lattice. This is usually done by giving up on the locality of the action, but other method exist. One of such model use a non-local derivative (SLAC derivative) that force the same momentum spectrum on the lattice than in the continuum[32]. This remove the doublers and restore Leibniz rule. Other similar method is to use a non-local product instead[33]. This model use the fermion doublers in the super-algebra, but result in an non-associative product. Both of the methods are successful for simple models, such as Wess-Zumino, however they are not successful for gauge theory yet. Lastly, a lattice gauge theory with full supersymmetry on the lattice have been realized by non-commutative formulation[28]. The problem of this last model is that it cannot be used for numerical simulations. Therefore while putting full supersymmetry on the lattice is very interesting from a theoretical point of view, but it has yet to create models usable for simulating supersymmetric Yang-Mills theories.

The last method is to preserve only partial supersymmetry on the lattice. With the use of topological twisting, it is possible to create nilpotent supercharges ($Q^2 = 0$). This allows us to keep a portion of the supersymmetry exact while giving up on the rest. It was shown that the presence the partial symmetry allows the restoration of the full supersymmetry in the continuum without any fine-tunning in low dimension [2][24]. The earliest use of this method to create a supersymmetric gauge theory was done by Kaplan [21]. The method was then refined by Sugino, who used link variables and topological twisting together to create his lattice supersymmetric Yang-Mills models.

2 Lattice simulation of $\mathcal{N} = (8, 8)$ SYM in two dimensions

The method developed by Sugino at al.[24][25] allows to create lattice SYM models keeping some of its supercharges intact. It was shown by perturbation theory that keeping only a few supercharges intact on the lattice is sufficient to assure the restoration of the full supersymmetry in the continuum limit in low dimension.

There are 2 main problems arising when putting SUSY on the lattice: the breaking of the Leibniz rule and the emergence of fermions doublers. Those issues brought foward many possible solutions, from giving up SUSY on the lattice to modifying the basic properties of the theory (locality, associativity,...) in order to make SUSY fit exactly on the lattice.

The approach used for the model in this study is to keep only partial SUSY on the lattice. Using a topological twist, 2 of the supercharges are made nilpotent and thus can be put on the lattice even if the Leibniz rule is broken. By a smart definition of the field and divergence operator it is possible to kill the fermion doublers (but hermiticity is broken in the fermionic sector).

In this section we present the gauge model used for our simulations. First, we present the continuum action and rewrite it in a $Q_{\pm}$-exact form. Next, we build the lattice action followed by some considerations about the formulation to make it useful for simulations.

[2]No fine tunning is needed for super Yang-Mills in one or two dimensions, starting in 3 dimensions one or more parameters are needed depending on the number of supersymmetries[24].

Some issues and properties that could limit the simulations are discussed in section 2.3. Lastly we state the simulations details.

2.1 Continuum theory

The Euclidean action of $\mathcal{N} = (8, 8)$ super Yang-Mills theory in 2 dimensions is given by

$$S = \frac{N}{\lambda} \int \mathrm{d}^2x \ \mathrm{tr}\Big\{ \frac{1}{4} F_{\mu\nu}^2 + \frac{1}{2}(D_\mu X_i)^2 - \frac{1}{4}[X_i, X_j]^2 + \frac{1}{2}\Psi_\alpha D_0 \Psi_\alpha - \frac{i}{2}\Psi_\alpha (\gamma_1)_{\alpha\beta} D_1 \Psi_\beta + \frac{1}{2}\Psi_\alpha (\gamma_i)_{\alpha\beta}[X_i, \Psi_\beta] \Big\}. \tag{6}$$

It contain two gauge fields $X_\mu (\mu = 0, 1)$, eight scalar fields $X_i (i = 2, 3 \cdots, 9)$, and sixteen fermions $\Psi_\alpha (\alpha = 1, 2, \cdots, 16)$. Every fields are written as matrices belonging to the $SU(N)$ group and can be decomposed as $\varphi = \sum_a \varphi^a T^a$ where T^a are the $SU(N)$ group generators, $\mathrm{tr}(T^a T^b) = \delta_{ab}$. The field strength is $F_{01} = \partial_0 X_1 - \partial_1 X_0 + i[X_0, X_1]$ and the covariant derivatives are defined by $D_\mu \varphi = \partial_\mu \varphi + i[X_\mu, \varphi]$. The gamma matrices $\gamma_a (a = 1, \cdots, 9)$ are chosen real and symmetric and satisfy the nine-dimensional Euclidean Clifford algebra, $\{\gamma_a, \gamma_b\} = 2\delta_{ab}$.

This action can be obtained from dimensional reduction of the $D = 10$, $\mathcal{N} = 1$ SYM theory. In ten dimension, the Majonara-Weyl condition reduce the fermionic degrees of freedom from 32 to 16, thus the usage of the nine-dimensional gamma matrices.

This action have only one free parameter, the "'t Hooft coupling λ as an overall constant, the symmetries of the theory forbid any other parameter. As symmetry, we have the 2D euclidean group, the $SO(8)$ rotation between the scalar fields, the gauge symmetry and supersymmetry on shell. The $SO(8)$ rotation symmetry is the left-over from the rotation in the reduced eight dimension from the ten dimensions theory. This rotation do not only affect the boson scalars but also the fermion fields. The $SU(N)$ gauge group is considered instead of the $U(N)$ group since the $U(1)$ part decouple from the theory and it is simpler to treat it independently. The supersymmetry of the action consist in the following 16 transformations,

$$Q_\alpha X_\mu = -i(\gamma_\mu)_{\alpha\beta} \Psi_\beta, \tag{7}$$

$$Q_\alpha X_i = -i(\gamma_i)_{\alpha\beta} \Psi_\beta, \tag{8}$$

$$Q_\alpha \Psi_\beta = i(\gamma_1)_{\alpha\beta} F_{01} + (\gamma_\mu \gamma_i)_{\alpha\beta} D_\mu X_i + \frac{i}{2}(\gamma_i \gamma_j)_{\alpha\beta}[X_i, X_j], \tag{9}$$

where $\gamma_0 = i$. The gauge transformations are defined as

$$\delta_\omega A_\mu = -D_\mu \omega, \qquad \delta_\omega \varphi = -i[\varphi, \omega], \tag{10}$$

where X_μ are the gauge fields and φ represent a scalar or a fermion field.

In order to obtain the Sugino lattice formulation we rewrite the action in an Q_+-exact form constructed with nilpotent supercharge using a topological twist. Both notation are equivalent and differ only by a renaming of the fields [3]. The action in Q_+-exact form is

[3] See appendix A.1 for the relation between both notations.

given by

$$S = Q_+Q_-\frac{N}{2\lambda}\int \mathrm{d}^2x\ \mathrm{tr}\Big\{ -4iB_iF^+_{i3} - \frac{2}{3}\epsilon_{ijk}B_iB_jB_k \\ - \psi_{+\mu}\psi_{-\mu} - \chi_{+i}\chi_{-i} - \frac{1}{4}\eta_+\eta_-\Big\}. \tag{11}$$

where μ runs from 0 to 3, i,j,k from 0 to 2. ϵ_{ijk} is a totally antisymmetric tensor satisfying $\epsilon_{012}=1$. The two gauge fields are renamed to $A_\mu(\mu=0,1)$, the scalar fields are separated into six real scalar fields A_2, A_3, B_i, C, and two complex scalar fields $\phi_\pm$. The fermions are given by $\psi_{\pm\mu},\ \chi_{\pm i},\ \eta_\pm$. The F^+_{i3} are extended field strength

$$F^+_{i3} = \frac{1}{2}\left(F_{i3} + \frac{1}{2}\epsilon_{ijk}F_{jk}\right), \tag{12}$$

$$F_{\mu\nu} = \partial_\mu A_\nu - \partial_\nu A_\mu + i[A_\mu, A_\nu], \tag{13}$$

with $\partial_\mu = 0$ for $\mu = 2,3$. This action is a dimensional reduced form of the four dimensional $\mathcal{N}=4$ SYM which has a well known topological twist[34].

The supercharges $Q_\pm$ are obtained with the following twist of the original supercharges

$$Q_+ = \frac{1}{\sqrt{2}}(Q_5 + iQ_{13}), \tag{14}$$

$$Q_- = \frac{1}{\sqrt{2}}(Q_1 + iQ_9). \tag{15}$$

The $Q_\pm$-transformations are nilpotent up to gauge transformations: $Q^2_\pm = i\delta_{\phi_\pm}$ and $\{Q_+, Q_-\} = -i\delta_C$. The associated $Q_\pm$-transformations are

$$\begin{array}{lll} Q_\pm A_\mu = \psi_{\pm\mu} & Q_\pm\psi_{\pm\mu} = -iD_\mu\phi_\pm, & Q_\pm\psi_{\mp\mu} = \frac{i}{2}D_\mu C \pm \tilde{H}_\mu, \\ Q_\pm B_i = \chi_{\pm i}, & Q_\pm\chi_{\pm i} = [B_i,\phi_\pm], & Q_\pm\chi_{\mp i} = \frac{1}{2}[C,B_i] \pm H_i, \\ Q_\pm C = \eta_\pm, & Q_\pm\eta_\pm = [C,\phi_\pm], & Q_\pm\eta_\mp = [\phi_\mp,\phi_\pm], \\ Q_\pm\phi_\pm = 0, & Q_\pm\phi_\mp = \eta_\mp, & \end{array}$$

$$\begin{aligned} Q_\pm H_i &= \pm\Big([\chi_{\mp i},\phi_\pm] + \frac{1}{2}[\chi_{\pm i}, C] + \frac{1}{2}[B_i,\eta_\pm]\Big), \\ Q_\pm\tilde{H}_\mu &= \pm\Big([\psi_{\mp\mu},\phi_\pm] + \frac{1}{2}[\psi_{\pm\mu}, C] - \frac{i}{2}D_\mu\eta_\pm\Big). \end{aligned} \tag{16}$$

$\tilde{H}_\mu$ and H_i are auxiliary field introduced to define $Q_\pm$ as closed transformations.

2.2 Lattice theory

For the lattice version of this theory, we prepare a 2D lattice of N_t sites in the temporal direction and N_x sites in the spacial one. The lattice spacing is a and, for simplicity, we set $(a=1)$ when the lattice spacing is not explicitly needed. The lattice sites are labeled by integers

$$\vec{x} = (t,x) \qquad t = 1,\cdots,N_t, \qquad x = 1,\cdots,N_x. \tag{17}$$

The fields of the theory are all placed on the sites with the exception of the gauge fields. The gauges fields are represented by link variables on the lattice

$$U_\mu(\vec{x}) = e^{iA_\mu(\vec{x})}. \tag{18}$$

Periodic boundary conditions are imposed on the boson fields. The fermions satisfy periodic boundary conditions in the spacial direction and anti-periodic boundary conditions in the temporal direction in order to account for the effect of finite temperature in the simulations.

The lattice gauge transformations for an infinitesimal transformation with the parameter $\omega(\vec{x})$ defined on the sites, are given by

$$\delta_\omega U_\mu(\vec{x}) = i\omega(\vec{x})U_\mu(\vec{x}) - iU_\mu(\vec{x})\omega(\vec{x}+\hat{\mu}), \qquad \delta\varphi(\vec{x}) = -i[\varphi(\vec{x}), \omega(\vec{x})], \tag{19}$$

where φ represent any field placed on a site. $\hat{\mu}$ is a unit vector in μ-direction.The forward and backward covariant difference operators are given by

$$\nabla^+_\mu \varphi(\vec{x}) = U_\mu(\vec{x})\varphi(\vec{x}+\hat{\mu})U^\dagger_\mu(\vec{x}) - \varphi(\vec{x}), \tag{20}$$

$$\nabla^-_\mu \varphi(\vec{x}) = \varphi(\vec{x}) - U^\dagger_\mu(\vec{x}-\hat{\mu})\varphi(\vec{x}-\hat{\mu})U_\mu(\vec{x}-\hat{\mu}), \tag{21}$$

respectively.

Some modifications are needed for the lattice counterparts of the $Q_\pm$-transformations in order to keep the supercharges nilpotent on the lattice. The cause of this effect is the use of link variable, thus the modifications are only needed for the field associated with the directions $\mu = 0, 1$. The modified $Q_\pm$-transformations for them are

$$\begin{aligned}
&Q_\pm U_\mu = i\psi_{\pm\mu}U_\mu,\\
&Q_\pm \psi_{\pm\mu} = -i\nabla^+_\mu\phi_\pm + i\psi_{\pm\mu}\psi_{\pm\mu},\\
&Q_\pm \psi_{\mp\mu} = \frac{i}{2}\nabla^+_\mu C \pm \tilde{H}_\mu + \frac{i}{2}\{\psi_{+\mu}, \psi_{-\mu}\},\\
&Q_\pm \tilde{H}_\mu = \pm\Big(\left[\psi_{\mp\mu}, \phi_\pm + \tfrac{1}{2}\nabla^+_\mu\phi_\pm\right] + \frac{1}{2}\left[\psi_{\pm\mu}, C + \tfrac{1}{2}\nabla^+_\mu C\right]\\
&\qquad\qquad - \frac{i}{2}\nabla^+_\mu\eta_\pm + \frac{1}{4}[\psi_{\pm\mu}, \{\psi_{+\mu}, \psi_{-\mu}\} \pm 2i\tilde{H}_\mu]\Big).
\end{aligned} \tag{22}$$

With the definitions above, we have $Q^2_\pm = i\delta_{\phi_\pm}$ and $\{Q_+, Q_-\} = -i\delta_C$ even on the lattice[24].

From the $Q_\pm$-exact action (11), we need to replace the integral with a summation over the sites and modify the field strengths in order to get the lattice formulation

$$\begin{aligned}
S = Q_+Q_- \frac{N}{2\lambda_0}\sum_{t,x}\ \mathrm{tr}\Big\{ &-4iB_iF^+_{i3} - \frac{2}{3}\epsilon_{ijk}B_iB_jB_k\\
&- \psi_{+\mu}\psi_{-\mu} - \chi_{+i}\chi_{-i} - \frac{1}{4}\eta_+\eta_-\Big\}.
\end{aligned} \tag{23}$$

The extended field strengths include both forward and backward covariant derivative,

$$F^+_{03} = \tfrac{1}{2}(\nabla^+_0 A_3 + \nabla^+_1 A_2), \tag{24}$$

$$F^+_{13} = \tfrac{1}{2}(\nabla^-_1 A_3 - \nabla^-_0 A_2), \tag{25}$$

$$F^+_{23} = \tfrac{1}{2}(i[A_2, A_3] + F_{01}), \tag{26}$$

so that the fermion doubler are killed.

On the lattice, the field strength F_{01} is written using plaquette (P_{01}), a closed loop of four link fields

$$F_{01}(\vec{x}) = -\frac{i}{2}\left(P_{01}(\vec{x}) - P_{01}^{\dagger}(\vec{x}) - \frac{1}{N}\mathrm{tr}(P_{01}(\vec{x}) - P_{01}^{\dagger}(\vec{x}))\right), \tag{27}$$

$$P_{01}(\vec{x}) = U_0(\vec{x})U_1(\vec{x}+\hat{0})U_0^{\dagger}(\vec{x}+\hat{1})U_1^{\dagger}(\vec{x}). \tag{28}$$

See section 2.3 and [24] for more details. This choice of field strength give a traceless hermitian F_{01} to the first power which we need in the $Q_{\pm}$-exact form.

The free parameters of the lattice action are the 't Hooft coupling λ, the gauge group used and lattice size. For our simulation, we choose the 't Hooft coupling in function of the desired dimensionless temperature. The lattice coupling is

$$\lambda_0 = a^2\lambda = \frac{1}{(T_0 N_t)^2}. \tag{29}$$

By performing the $Q_{\pm}$-transformations of (23) we get the full lattice action. It is useful to define shifted fields notation

$$\varphi^{+\mu}(\vec{x}) = U_\mu(\vec{x})\varphi(\vec{x}+\hat{\mu})U_\mu^{\dagger}(\vec{x}), \qquad (\mu = 0,1), \tag{30}$$

$$\varphi^{-\mu}(\vec{x}) = U_\mu^{\dagger}(\vec{x}-\hat{\mu})\varphi(\vec{x}-\hat{\mu})U_\mu(\vec{x}-\hat{\mu}), \qquad (\mu = 0,1), \tag{31}$$

$$\varphi^{\pm\mu}(\vec{x}) = \varphi(\vec{x}), \qquad (\mu = 2,3) \tag{32}$$

and the covariant derivative are defined in dimension 0 to 3

$$\nabla_\mu^{\pm}\varphi = \pm(\varphi^{\pm\mu} - \varphi), \qquad (\mu = 0,1), \tag{33}$$

$$\nabla_\mu^{\pm}\varphi = i[A_\mu, \varphi], \qquad (\mu = 2,3). \tag{34}$$

The lattice action has two complex covariant difference operators,

$$\nabla_\mu^{+\nu}\varphi = \frac{1}{2}(\varphi^{+\mu}P_{\mu\nu} + P_{\nu\mu}\varphi^{+\mu} - \varphi P_{\nu\mu} - P_{\mu\nu}\varphi), \tag{35}$$

$$\nabla_\mu^{-\nu}\varphi = \frac{1}{2}(P_{\nu\mu}\varphi + \varphi P_{\mu\nu} - P_{\mu\nu}^{-\mu}\varphi^{-\mu} - \varphi^{-\mu}P_{\nu\mu}^{-\mu}), \tag{36}$$

for $\mu, \nu = 0, 1, \mu \neq \nu$.

The boson part of the lattice action is

$$\begin{aligned} S_B = \frac{N}{2\lambda_0}\sum_{t,x}\mathrm{tr}\Big\{ & \frac{1}{4}[\phi_+,\phi_-]^2 + \frac{1}{4}[C,\phi_+][C,\phi_-] - \frac{1}{4}[C,B_i]^2 \\ & -\nabla_\mu^+\phi_+\nabla_\mu^+\phi_- + [B_i,\phi_+][B_i,\phi_-] + \frac{1}{4}(\nabla_\mu^+ C)^2 \\ & +(H_i + i\varphi_i)^2 + \varphi_i^2 + (\tilde{H}_\mu + iG_\mu)^2 + G_\mu^2 \Big\}, \end{aligned} \tag{37}$$

where φ_i and G_μ are given by

$$\varphi_0 = \nabla_0^+ A_3 + \nabla_1^+ A_2 - i[B_1, B_2], \tag{38}$$
$$\varphi_1 = \nabla_1^- A_3 - \nabla_0^- A_2 - i[B_2, B_0], \tag{39}$$
$$\varphi_2 = i[A_2, A_3] + F_{01} - i[B_0, B_1], \tag{40}$$
$$G_0 = i[A_3^{+0}, B_0] - i[A_2, B_1^{+0}] + \nabla_1^{-0} B_2, \tag{41}$$
$$G_1 = i[A_2^{+1}, B_0] + i[A_3, B_1^{+1}] - \nabla_0^{-1} B_2, \tag{42}$$
$$G_2 = -\nabla_1^- B_0 + \nabla_0^+ B_1 + i[A_3, B_2], \tag{43}$$
$$G_3 = -\nabla_0^- B_0 - \nabla_1^+ B_1 - i[A_2, B_2]. \tag{44}$$

The boson action is semi positive definite. The auxiliary fields $\tilde{H}_\mu$ and H_i can be integrated using a Gaussian integral. The action is similar to the continuum action with the exception of the shift in the fields composing φ_i and G_μ.

The fermion part of the action is given by

$$\begin{aligned}
S_F = \frac{N}{2\lambda_0} \sum_{t,x} \mathrm{tr} \Big\{ & \frac{1}{4}\eta_+[\phi_-, \eta_+] + \chi_{+i}[\phi_-, \chi_{+i}] + \psi_{+\mu}[\tfrac{1}{2}(\phi_- + \phi_-^{+\mu}), \psi_{+\mu}] \\
& + \frac{1}{4}\eta_-[\phi_+, \eta_-] + \chi_{-i}[\phi_+, \chi_{-i}] + \psi_{-\mu}[\tfrac{1}{2}(\phi_+ + \phi_+^{+\mu}), \psi_{-\mu}] \\
& - \frac{1}{4}\eta_+[C, \eta_-] + \chi_{+i}[C, \chi_{-i}] + \psi_{+\mu}[\tfrac{1}{2}(C + C^{+\mu}), \psi_{-\mu}] \\
& - \eta_-[B_i, \chi_{+i}] - \eta_+[B_i, \chi_{-i}] + 2\epsilon_{ijk}\chi_{-i}[B_j, \chi_{+k}] \\
& - i\nabla_\mu \eta_+ \psi_{-\mu} - i\nabla_\mu \eta_- \psi_{+\mu} + [A_\mu, \eta_+]\psi_{-\mu} + [A_\mu, \eta_-]\psi_{+\mu} \\
& - 2\chi_{+0}(+i\nabla_0^+ \psi_{-3} + i\nabla_1^+ \psi_{-2} + [A_2^{+1}, \psi_{-1}] + [A_3^{+0}, \psi_{-0}]) \\
& + 2\chi_{-0}(+i\nabla_0^+ \psi_{+3} + i\nabla_1^+ \psi_{+2} + [A_2^{+1}, \psi_{+1}] + [A_3^{+0}, \psi_{+0}]) \\
& - 2\chi_{+1}(-i\nabla_0^- \psi_{-2} + i\nabla_1^- \psi_{-3} - [A_2^{-0}, \psi_{-0}^{-0}] + [A_3^{-1}, \psi_{-1}^{-1}]) \\
& + 2\chi_{-1}(-i\nabla_0^- \psi_{+2} + i\nabla_1^- \psi_{+3} - [A_2^{-0}, \psi_{+0}^{-0}] + [A_3^{-1}, \psi_{+1}^{-1}]) \\
& - 2\chi_{+2}(+i\nabla_0^{+1} \psi_{-1} - i\nabla_1^{+0} \psi_{-0} - [A_2, \psi_{-3}] + [A_3, \psi_{-2}]) \\
& + 2\chi_{-2}(+i\nabla_0^{+1} \psi_{+1} - i\nabla_1^{+0} \psi_{+0} - [A_2, \psi_{+3}] + [A_3, \psi_{+2}]) \\
& - 2\psi_{-3}[B_0^{-0}, \psi_{+0}^{-0}] - 2\psi_{-3}[B_1^{+1}, \psi_{+1}] - 2\psi_{-3}[B_2, \psi_{+2}] \\
& + 2\psi_{+3}[B_0^{-0}, \psi_{-0}^{-0}] + 2\psi_{+3}[B_1^{+1}, \psi_{-1}] + 2\psi_{+3}[B_2, \psi_{-2}] \\
& - 2\psi_{-2}[B_0^{-1}, \psi_{+1}^{-1}] + 2\psi_{-2}[B_1^{+0}, \psi_{+0}] \\
& + 2\psi_{+2}[B_0^{-1}, \psi_{-1}^{-1}] - 2\psi_{+2}[B_1^{+0}, \psi_{-0}] \\
& - i\psi_{-0}[A_3^{+0}, [B_0, \psi_{+0}]] - i\psi_{-0}[B_0, [A_3^{+0}, \psi_{+0}]] \\
& - i\psi_{-0}[A_2, [B_1^{+0}, \psi_{+0}]] - i\psi_{-0}[B_1^{+0}, [A_2, \psi_{+0}]] \\
& + i\psi_{-1}[A_3, [B_1^{+1}, \psi_{+1}]] + i\psi_{-1}[B_1^{+1}, [A_3, \psi_{+1}]] \\
& - i\psi_{-1}[A_2^{+1}, [B_0, \psi_{+1}]] - i\psi_{-1}[B_0, [A_2^{+1}, \psi_{+1}]] \\
& + \mathcal{L}_P - \frac{1}{4}\sum_{\rho=0,1} \{\psi_{+\rho}, \psi_{-\rho}\}^2 \Big\},
\end{aligned} \tag{45}$$

with

$$\begin{aligned}\mathcal{L}_P =&\frac{1}{2}\psi_{-0}\left\{(P_{10}B_2 - B_2P_{01})^{-1} + B_2P_{10} - P_{01}B_2, \psi_{+0}\right\}\\ &+ \psi_{-0}P_{01}\psi^{+1}_{+0}B_2 - \psi_{-0}B_2\psi^{+1}_{+0}P_{10} + \psi^{+1}_{-0}B_2\psi_{+0}P_{01} - \psi^{+1}_{-0}P_{10}\psi_{+0}B_2\\ &- \frac{1}{2}\psi_{-1}\left\{(P_{01}B_2 - B_2P_{10})^{-1} + B_2P_{01} - P_{10}B_2, \psi_{+1}\right\}\\ &- \psi_{-1}P_{10}\psi^{+0}_{+1}B_2 + \psi_{-1}B_2\psi^{+0}_{+1}P_{01} - \psi^{+0}_{-1}B_2\psi_{+1}P_{10} + \psi^{+0}_{-1}P_{01}\psi_{+1}B_2\\ &+ \psi_{-0}P_{01}\psi_{+1}B_2 - \psi_{-0}B_2\psi_{+1}P_{10} + \psi^{+1}_{-0}P_{10}B_2\psi_{+1} - \psi^{+1}_{-0}\psi_{+1}B_2P_{01}\\ &- \psi_{-0}\psi^{+0}_{+1}P_{01}B_2 + \psi_{-0}B_2P_{10}\psi^{+0}_{+1} + \psi^{+1}_{-0}B_2\psi^{+0}_{+1}P_{01} - \psi^{+1}_{-0}P_{10}\psi^{+0}_{+1}B_2\\ &- \psi_{-1}P_{10}\psi_{+0}B_2 + \psi_{-1}B_2\psi_{+0}P_{01} - \psi^{+0}_{-1}P_{01}B_2\psi_{+0} + \psi^{+0}_{-1}\psi_{+0}B_2P_{10}\\ &+ \psi_{-1}\psi^{+1}_{+0}P_{10}B_2 - \psi_{-1}B_2P_{01}\psi^{+1}_{+0} - \psi^{+0}_{-1}B_2\psi^{+1}_{+0}P_{10} + \psi^{+0}_{-1}P_{01}\psi^{+1}_{+0}B_2.\end{aligned} \tag{46}$$

In the naive continuum limit, the complicated term $\mathcal{L}_P$ becomes two simple terms,

$$\mathcal{L}_P = -2\psi_{-1}[B_2, \psi_{+0}] + 2\psi_{-0}[B_2, \psi_{+1}], \tag{47}$$

while the shifts of fields in (45) disappears. Thus the fermionic part of the lattice action is equivalent to the continuum version.

This lattice action have four-fermions interaction terms

$$S_{4f} = \frac{N}{2\lambda_0}\sum_{t,x}\sum_{\rho=0,1}\mathrm{tr}\left(-\frac{1}{4}\{\psi_{+\rho}, \psi_{-\rho}\}^2\right). \tag{48}$$

While these terms disappear in the continuum limit, they are needed to keep that supersymmetry exact at finite lattice spacing. It is not possible to treat four-fermi interaction directly in the simulation, therefore we insert auxiliary fields

$$S_{4f} = \frac{N}{2\lambda_0}\sum_{t,x}\sum_{\rho=0,1}\mathrm{tr}\left(\sigma_\rho^2 + \psi_{+\rho}[\sigma_\rho, \psi_{-\rho}]\right). \tag{49}$$

In this form, these interactions can be treated with the other fermion terms.

Fermion doublers

Fermions on the lattice normally have extra degrees of freedom from the fact that their action contain only a first derivative. Since SUSY requires the same number of degree of freedom between the bosons and fermions, this issue must be addressed. The action used is written using a mixture of backward and forward different operator arranged in a way to create a non hermitian Dirac operator D. This formulation is equivalent to adding a Wilson mass to the fermions

$$\nabla^+_\mu = \frac{\nabla^+_\mu + \nabla^-_\mu}{2} + \frac{a}{2}\nabla^+_\mu\nabla^-_\mu \tag{50}$$

This breaks chirality but allows us to evade the lattice No-Go that shows that the doublers are needed on the lattice. To do the numerical simulation, a hermitian Dirac operator is needed so $D^\dagger D$ is used. The present arrangement of backward and forward operator

is chosen such that the kinetic part of $D^\dagger D$ if composed of second derivative, killing the fermion doublers.

The fermionic part of the action can be written as

$$S_F \propto \Psi^T D \Psi \tag{51}$$

Looking at the kinetic part of the Dirac operator, we have [4]

$$D = \begin{bmatrix} 0 & -iK^T \\ iK & 0 \end{bmatrix} \tag{52}$$

with

$$K = \begin{bmatrix} 0 & 0 & 0 & 0 & 0 & 0 & \nabla_1^- & \nabla_0 \\ 0 & 0 & 0 & 0 & 0 & 0 & -\nabla_0^- & \nabla_1 \\ 0 & 0 & 0 & 0 & -\nabla_1^- & \nabla_0 & 0 & 0 \\ 0 & 0 & 0 & 0 & -\nabla_0^- & -\nabla_1 & 0 & 0 \\ 0 & 0 & \nabla_1 & \nabla_0 & 0 & 0 & 0 & 0 \\ 0 & 0 & -\nabla_0^- & \nabla_1^- & 0 & 0 & 0 & 0 \\ -\nabla_1 & \nabla_0 & 0 & 0 & 0 & 0 & 0 & 0 \\ \nabla_0^- & \nabla_1^- & 0 & 0 & 0 & 0 & 0 & 0 \end{bmatrix}. \tag{53}$$

The hermitian form of the fermion operator ($D^\dagger D$) is diagonal and composed of a second derivative

$$D^\dagger D \propto -\nabla_0 \nabla_0^- - \nabla_1^- \nabla_1. \tag{54}$$

This way, the Dirac operator does not create fermion doublers.

2.3 Validity of the lattice action

In this section, we examine a few concerns about the action. We begin by commenting on the flat direction present in the action. Then we discuss about the continuum limit of the lattice action. With the present action, there is two issues arising when taking the continuous limit. First the lattice action have a degenerate vacua issue from the fields strength term. Also, there is some cross-terms that are not cancelling each other properly at finite lattice spacing.

Flat direction The bosonic action (6) has a known flat direction. This case arise when the scalar fields are non-zero but commute to each other, that way they do not contribute to the action. This correspond to every scalar field being diagonal and constant, up to a gauge transformation,

$$A_\mu = 0, \quad X_i = \text{constant and diagonal matrices.} \tag{55}$$

In this case, the fields can take arbitrarily big values. The size of the fields, given by $R^2 = \sum \text{tr}(X_i^2)$, is unbounded. This is problematic for simulations because the fields

[4] This exact notation depends on the ordering of the fermion fields. Here we use the twisted field in the order $\psi_{+\mu}, \chi_{+i}\eta_+/2, \psi_{-\mu}, \chi_{i-}\eta_-/2$ with the μ and i in ascending order.

do not stays around one vacuum and move freely, making it hard to measure anything with a reasonable accuracy. There is also the question if these configurations have any physical meaning. To remove the instability, we can add a mass term[39] to the action

$$S_{mass} = \frac{N}{2\lambda_0} \sum_{t,x} \sum_{i=2}^{9} m_0^2 \ \mathrm{tr}(X_i^2), \tag{56}$$

where $m_0 = ma$ is the dimensionless mass. However, this mass breaks supersymmetry. A controllable SUSY breaking term can be useful in some situations but in most cases we want to keep the symmetry.

The flat direction is naturally suppressed in some parameter range such as at high temperature or with a high N. A simple explanation of this suppression is that the flat direction take the form of a valley in the configuration space. When the boson coefficient $N/\lambda_0 = NN_t^2T^2$ increase, the valley get thinner and the configurations are less likely to stay inside. Thus at high temperature, big group $SU(N)$ or close to the continuum (high N_t) the flat direction are suppressed. A suppression also arises at high lattice volume (N_t or N_x) because in this situations, constant configurations are less probable.

Continuous limit When taking the naive continuous limit $a \to 0$, we expect that the fields and constants scale in accord with their unit. The 't Hooft coupling λ, which is the scale of the model, has a mass dimension of two. Thus, the continuum limit is realized by taking $\lambda_0 (= \lambda a^2) \to 0$ with fixed λ. For the scalar, fermions and auxiliary fields we have

$$X_i^{lat.} = aX_i^{cont.}, \qquad \Psi^{lat.} = a^{3/2}\Psi^{cont.}, \qquad H_a^{lat.} = a^2 H_a^{cont.}. \tag{57}$$

Here, we have the X_i representing the eight scalar fields, Ψ the fermion fields and H_a the seven auxiliary fields. The *lat.* symbol indicate the lattice version of the fields which are dimensionless, while *cont.* indicate the continuum one with proper units. For the gauge related fields, we expect

$$U_\mu^{lat.} = e^{iaA_\mu^{cont.}} \approx 1 + iaA_\mu^{cont.}, \qquad P_{01}^{lat.} = e^{ia^2 F_{01}^{cont.}} \approx 1 + ia^2 F_{01}^{cont.}, \tag{58}$$

Using these relations, we can show that the lattice action is equivalent to continuum one. This said, the action posses lattice artifact that might not disappear in simulations.

Plaquette artifacts The first issue when taking the continuum limit is a degenerate vacua issue that arise from the choice of F_{01} (27). It is known that this simple choice of constructing the field strength could be problematic[22]. Keeping only the gauge fields and setting every other fields to zero, the action becomes

$$S_B|_{X_i=0} = \frac{N}{2\lambda_0} \sum_{t,x} \mathrm{tr} \left\{ -\frac{1}{4} \left(P_{01} - P_{01}^\dagger - \frac{1}{N} \mathrm{tr}(P_{01} - P_{01}^\dagger) \right)^2 \right\}. \tag{59}$$

This action have the expected $\frac{1}{N}\mathrm{tr}P_{01} \approx 1 + i\frac{1}{N}\mathrm{tr}F_{01}$ solution, but it also has solution in the form of $\frac{1}{N}\mathrm{tr}P_{01} \approx -1 + i\frac{1}{N}\mathrm{tr}F_{01}$. In the SU(2) case, this is obtained by $P_{01} = -1$, but is has more varied solutions for bigger group. When the field configuration is around an

extra vacuum, our expected relation between lattice and continuum field (58) is invalid. Thus we cannot trust our simulation to give valid results. To remove these extra vacua, one can use a $\tan(\theta/2)$-type field tensor[26] or an admissibility-type field tensor[23]

$$F_{01}(\vec{x}) = -\frac{i}{2}\frac{\left(P_{01}(\vec{x}) - P_{01}^{\dagger}(\vec{x}) - \frac{1}{N}\mathrm{tr}(P_{01}(\vec{x}) - P_{01}^{\dagger}(\vec{x}))\right)}{1 - \frac{1}{\epsilon^2}\mathrm{tr}(2 - P_{01} - P_{10})}. \tag{60}$$

Here, an admissibility condition limit the size of the variation of P_{01} to the order of the parameter ϵ. While this definition of the field strength is an effective way to assure the correspondence of the lattice action with the continuum one, they are hard to use in numerical simulations.

Here, we argue that it is simpler and more efficient to use the simplest form (27) when doing numerical simulation for our purpose. Even with a lattice action that allow the extra vacua, if we keep the plaquette around 1 ($1/N\mathrm{tr}P_{01} = 1$) during the simulation, we have the proper continuum limit. In order to have the good minimum, we start our simulation from a cold configuration ($U_\mu = 1$) which corresponds to the desired minimum. Between this minimum and the artifacial minima, there is a potential barrier corresponding to the halfway point between the 2 minima, as shown in figure 4. At this point, the action (59) as a value of $N^2/2\lambda_0$ or $N^2TN_t^2/2$ in simulation parameter If this barrier is strong enough, transition between the minima is suppressed. Thus we can choose our simulation parameters so that we don't observe any transition in the simulation. While this seems to limit the range of parameters that can be simulated, it happens to be the same conditions in which the flat direction is suppressed. We already need to do the simulations under those conditions in the massless case. Therefore our choice of plaquette, without any admissibility condition to kill the extra vacua, is more efficient in this case. If someone desired to do the simulation at low temperature and small N, killing the flat direction with a mass that keep SUSY invariance[35], then the more complex field strength definition (60) might be preferable to the usage of very big lattice $N_t \approx 1/(T * N^2)$.

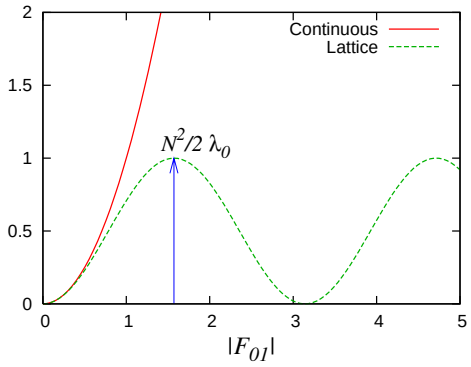

Figure 4: Action of the gauge field as a function of the magnitude of the gauge field ($|F_{01}| = \sqrt{1/N\mathrm{tr}F_{01}^2}$). The lattice action is consistent with the continuous one when the fields are small, but shows other minima. A "potential" wall with a height of $N^2/2\lambda_0$ suppress the transition between the minima.

Artifacts flat direction The second issue is the higher derivative terms. When looking at the lattice action (38), the main difference with the continuum action is inside the G_μ and φ_i terms. In the continuum action, the cross-terms from the square of G_μ and φ_i cancel each other, but on the lattice, because of the shifts, the cancellation is not exact.

The corresponding part of the action is

$$S = \frac{N}{2\lambda} \sum_{\vec{x}} (\varphi_i^2 + G_\mu^2). \tag{61}$$

Taking the continuum limit means that $\varphi_i,\ G_\mu\ \to 0$, but the cross-terms of G_μ and φ_i,

$$\begin{aligned}\Delta = \frac{N}{\lambda_0} \sum_{t,x} \mathrm{tr}\, \{ & iF_{01}[A_2, A_3] - \nabla_0^- A_2 \nabla_1^- A_3 + \nabla_0^+ A_3 \nabla_1^+ A_2 \\ & -iF_{01}[B_0, B_1] + \nabla_0^- B_0 \nabla_1^+ B_1 - \nabla_0^+ B_1 \nabla_1^- B_0 \\ & -i\nabla_0^- A_2[B_0, B_2] + i\nabla_0^- B_0[A_2, B_2] - i\nabla_0^{-1} B_2[A_2^{+1}, B_0] \\ & -i\nabla_0^+ A_3[B_1, B_2] + i\nabla_0^+ B_1[A_3, B_2] - i\nabla_0^{-1} B_2[A_3, B_1^{+1}] \\ & -i\nabla_1^+ A_2[B_1, B_2] + i\nabla_1^+ B_1[A_2, B_2] - i\nabla_1^{-0} B_2[A_2, B_1^{+0}] \\ & +i\nabla_1^- A_3[B_0, B_2] - i\nabla_1^- B_0[A_3, B_2] + i\nabla_1^{-0} B_2[A_3^{+0}, B_0] \\ & + [A_2, A_3][B_0, B_1] - [A_2^{+1}, B_0][A_3, B_1^{+1}] + [A_2, B_1^{+0}][A_3^{+0}, B_0] \} \,,\end{aligned} \tag{62}$$

are not positive definite by themselves. This means that there could possibly be configurations of the fields in which the cross-terms are big and negative, effectively canceling the main part of the boson action. This would create extra flat directions in the lattice formulation. The simulations are made in a way to suppress the flat directions of the continuum theory. Therefore we expect that the same suppression comes into play here. Thus we do not try to repair this possible problem, we simply measure the term Δ to verify that it is well behaved.

2.4 Simulation details

We did our simulations using the rational Hybrid Monte Carlo method[44]. This is a method used to obtain random boson field configurations whose probabilities are consistent with the simulation action, $P(C) \propto e^{-S(C)}$. In this method the field configuration move in the configurations space using Hamiltonian dynamics in a virtual time. The momentum of the field is randomized every 0.5 step in the virtual time, this represent one trajectory. Each trajectory is furthermore separated into smaller time step in which the dynamics are computed. At the end of each trajectory, a Metropolis step is done to correct the effect of the discretization of the Hamiltonian dynamics. The time steps are chosen to keep the acceptance rate over 80%. Moreover, the dynamical effects of the fermions are treated using the pseudo-fermion method. This only take into account the norm of the pfaffian, the phase can be reweighed in the result, but the numerical cost is great. Thus we only use the phase reweighing method for the smaller simulations.

The pseudo fermion method consist in integrating the fermion to get the pfaffian,

$$\mathrm{pf}(D) = \int \mathrm{D}\Psi \, \mathrm{e}^{-\Psi^T D \Psi}. \tag{63}$$

The matrix D is not hermitian and the pfaffian is complex. This is caused by the Majorana-Weyl nature of the fermion in $N = 1,\ D = 10$ SYM. To include the effects of the absolute value of the pfaffian we change it to a determinant by $\det(D) = \mathrm{pf}(D)^2$,

then we include pseudo fermions ϕ as

$$|\mathrm{pf}(D)| = \det(D^\dagger D)^{1/4}, \tag{64}$$

$$= \int D\phi^\dagger D\phi \, \exp\left\{-\phi^\dagger (D^\dagger D)^{-\frac{1}{4}}\phi\right\}. \tag{65}$$

The pseudo fermions are randomly generated at the beginning of each trajectory and kept constant until the next. The roots of the matrices are obtained with the rational approximation method

$$(D^\dagger D)^{-1/4} \simeq \alpha_0 + \sum_{i=1}^{N_r} \left(\frac{\alpha_i}{D^\dagger D + \beta_i}\right). \tag{66}$$

The inversions of $D^\dagger D + \beta_i$ is computed using the multiple shift conjugate gradient solver[36]. The parameters of the approximation (N_r, α_i and β_i) determine the range of the eigenvalues of $D^\dagger D$ in which the approximation is valid [37]. During the thermalization step of the simulation, we compute the maximum and minimum of the eigenvalues. From those results, we fix the parameters N_r, α_i, β_i of the main part of the simulation in a way to keep the accuracy of the approximation over 10^{-13}. When the calculation cost of the full pfaffian is not too great, we obtain the pfaffian directly in order to include the effect of the phase.

3 Confirmation of the validity of the simulation

In this work we use of Sugino's model for the two dimensional $\mathcal{N} = (8, 8)$ SYM theory. We need to confirm by the simulations that the model has the expected behavior. To do so, we first look at the issues discussed in section 2.3. Then we use the supersymmetric Ward-Takahashi identities to observe the restoration of the full supersymmetry in the continuum limit. Lastly, we compare our results with perturbative calculations in the high temperature limit.

3.1 Validity of the simulation

As explained in section 2.3, the lattice action has extra vacua and flat directions. The flat directions issue is expected to occur in a certain parameter region, and simulations presenting such behavior are simply considered invalid. As shown in figure 5, it is evident when a simulation enters into a flat direction. Without a mass term, for $N = 12$, we can only do simulation with a temperature higher than $T = 1$ using a small lattice of $N_t = 8$, $N_x = 8$. Doubling the size of the lattice to $N_t = 8$, $N_x = 16$ allows us to lower the temperature to $T = 0.3$, where we are limited by the computation of the fermions. This is actually a great advantage of simulations in two dimensions over simulations in one dimensions. In one dimensions, the group size (N) is usually increased to suppress the flat direction, whereas, in two dimensions, we have the choice to increase the space volume (N_x) instead. Increasing the group size leads to slower computation than increasing the lattice size [5].

[5]The increase of work load for a larger group size mostly treated in one processor, but the burden of an increase in the lattice size is easily shared between multiple processors.

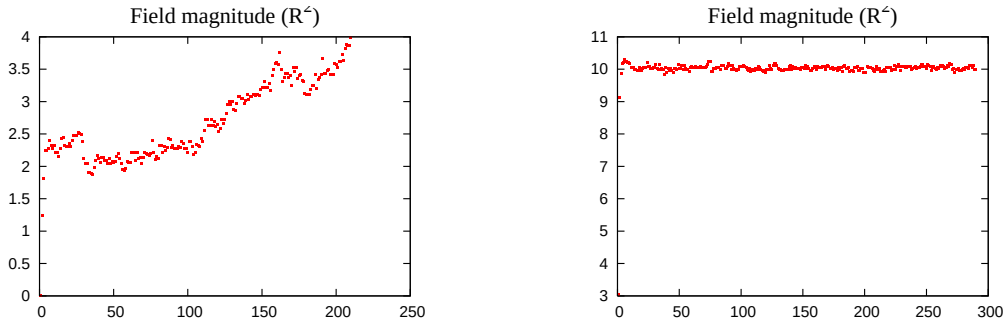

Figure 5: Size of the scalar fields $R^2 = \mathrm{tr}(X_i^2)$ as a function of the trajectory. The gauge group is $N = 12$ in both case. On the left, we have a smaller lattice $N_t = 8$, $N_x = 8$ at $T = 0.8$. On the right, the parameters are $N_t = 8$, $N_x = 16$ at $T = 0.3$. The simulation on the left have a flat direction problem.

Figure 6 and 7 shows the contributions of the higher derivative terms Δ (62). By removing the simulation with a flat direction problem, we should have removed case where those terms are problematic. As expected, for all parameters used, Δ is relatively small, only a few percent of the action. It does approaches zero as $a \to 0$ showing that this artifact do disappear in the continuum limit. From figure 6 we see that the presence of the mass is an efficient way to suppress Δ. Figure 7 shows that these term get larger at large coupling. At over 15% of the bosonic action, there may have some effects on the simulations. Contrary to the flat direction, a wider lattice does not reduce these terms.

Lastly, we look at the extra minima in the gauge fields sector. Every minima correspond to $\mathrm{tr}(P_{01})/N = 1$ or -1. By observing $\mathrm{tr}(P_{01})/N$ to make sure that it never goes negative, we can confirm that no transitions between minima occur. As can be seen in the histogram of $\mathrm{tr}(P_{01})/N$ (figure 8), the plaquettes value stay close to one. We can see that field strength approximation is improved in the coutinous limit as the plaquette are more concentrated around $\mathrm{tr}(P_{01})/N = 1$. Figure 9 shows the temperature dependence. At low temperature, the plaquette spread wider therefore bigger group or simulation closer to the continuum are needed when going to lower temperature. We never observed any negative values in any simulations used in this study [6]. Thus, we can conclude that the extra vacua do not affect our main results.

[6] We only observed such transition in very small lattice size such as $N_t = 4$, $N_x = 4$ with small group $N = 2, 3$.

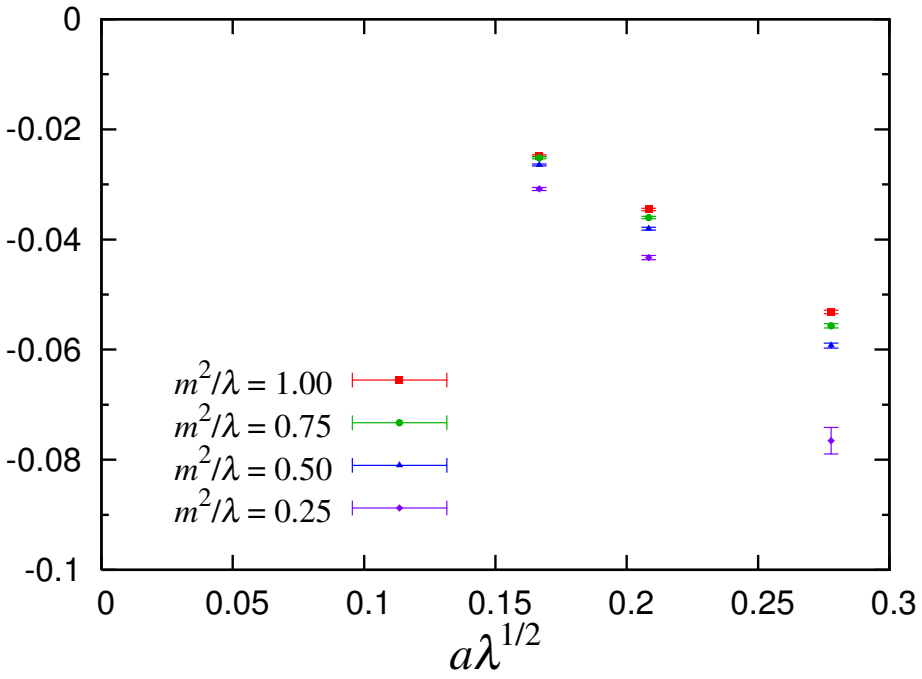

Figure 6: Higher derivative terms in the bosonic sector (Δ) against the lattice spacing. The vertical axis denotes Δ/S'_B where S'_B is the bosonic part of the action without the auxiliary fields σ_ρ. These terms are suppressed in the continuum limit.

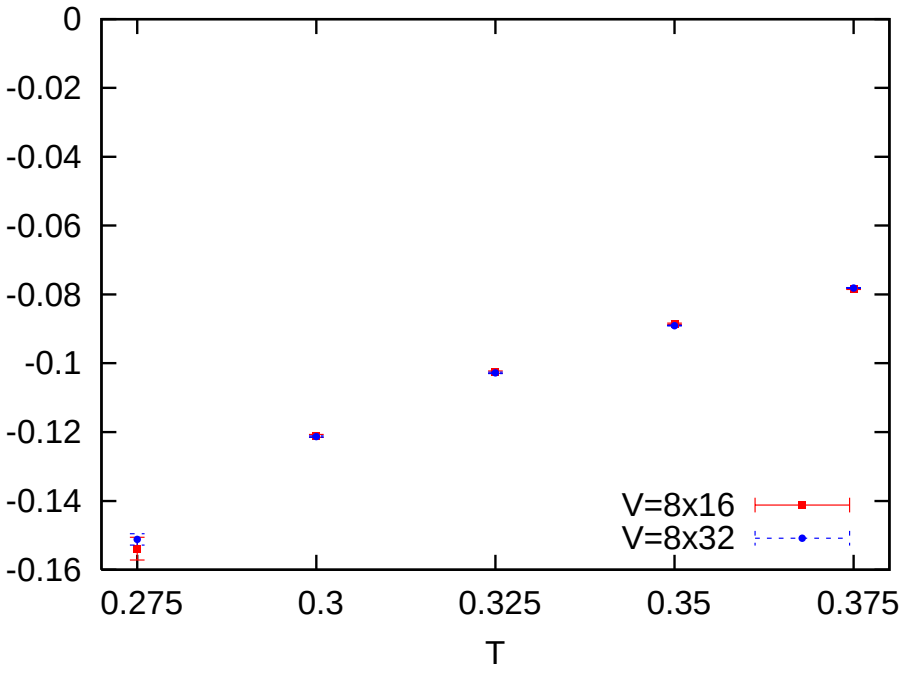

Figure 7: Importance of the higher derivative terms in the bosonic sector (Δ/S_B) as a function of the temperature. These simulation are massless, the group size is $N = 12$. Contraly to the original flat directions, the space volume (N_x) do not suppress the importance of (Δ). At low temperature, the artifact becomes important.

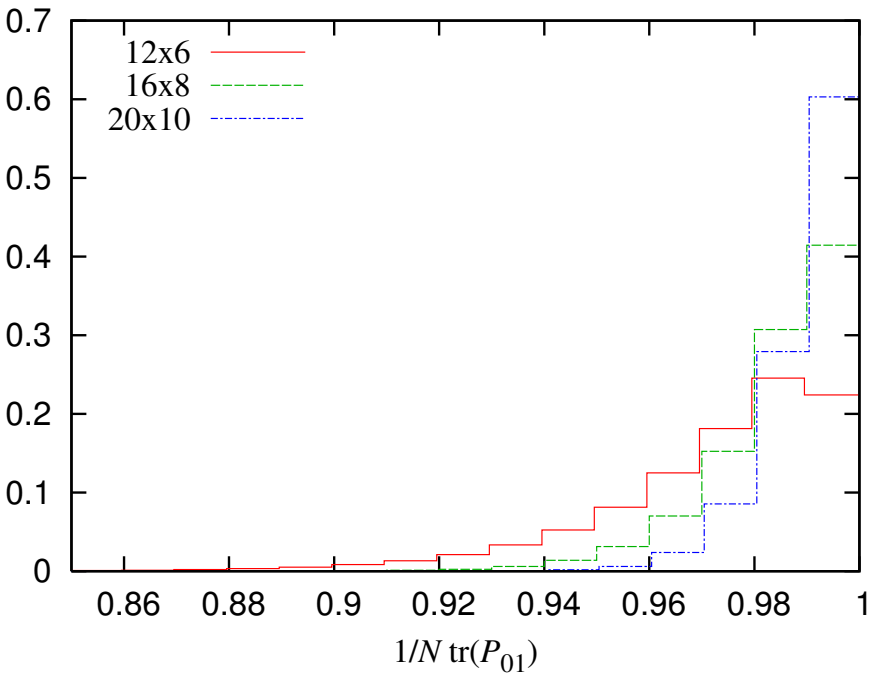

Figure 8: Histogram of the plaquettes $(\mathrm{tr}(P_{01})/N)$ for $m^2/\lambda = 0.25$. This includes all plaquettes of every configuration. As the lattice spacing approaches zero, the distribution is strongly localized at $P_{01} = 1$.

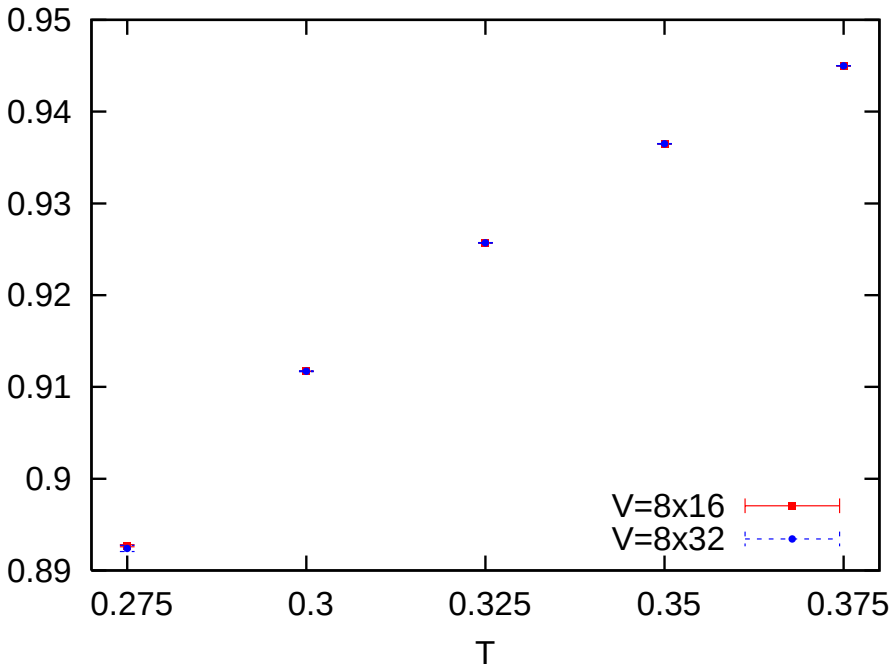

Figure 9: Average value of $\mathrm{tr}(P_{01})/N$ as a function of the temperature. The group size is $N = 12$ and there is no mass term in these simulations. At low temperature, the plaquettes take a wider range of values. At very low temperature transitions might occur limiting the temperature range of the present method. Increasing the volume in the space direction (N_x) do not affect the plaquettes value.

3.2 Recovery of the full supersymmetry

Looking at the restoration of SUSY in the continuum limit is needed To confirm the validity of the lattice formulation of the $2D$, $N = (8, 8)$ super Yang-Mills, we verify that the full supersymmetry is restored in the continuum limit. The finite lattice spacing break 14 of the 16 supersymmetries. It is not trivial that in the continuum limit all symmetries are present. supersymmetry is also broken by finite temperature effects. To isolate the lattice effect, we did our simulation at low temperature. We mesure the symmetry breaking using the supersymmetric Ward-Takahashi Identities(SWTI). These identities are valid regardless of the anti-periodic boundary condition imposed on the fermions. Therefore the symmetry breaking effect caused by the finite temperature can be ignored. Still, at high temperature, effective supersymmetry breaking terms dynamically appear, motivating the use of a low temperature for this part of the simulations.

We also include a mass term in those simulations. This mass stabilize the simulation by removing the flat direction problem arising at low temperature. The SUSY breaking effect of the mass is not a nuisance when looking at the restoration of the SUSY breaking, but is actually quite useful. Since this source of breaking is controllable, it is easily identified and can be isolated. Also, it allows a easier quantification of the breaking from the other source.

For these simulations we used a small group $SU(2)$. The dimensionless temperature is set at $T_{\text{eff}} = T/\lambda^{1/2} = 0.3$.

3.2.1 SUSY Ward-Takahashi identity

To observe the symmetry restoration, we use the Ward-Takahashi identity which include the breaking effect of the mass term (partially conserved supercurrent)[39]. To each symmetry of the action, there is an associated current that is conserved. The Ward-Takahashi identities represent the conservation law of this current. The current associated with supersymmetry is, in the continuum theory,

$$J_\mu = -\frac{N}{\lambda}\left\{\gamma_0\gamma_1\gamma_\mu \text{tr}(\Psi F_{01}) + \gamma_\nu\gamma_i\gamma_\mu \text{tr}(\Psi D_\nu X_i) + \frac{i}{2}\gamma_i\gamma_j\gamma_\mu \text{tr}(\Psi[X_i, X_j])\right\}. \tag{67}$$

With the SWTI being the conservation of the currents taking the form of

$$\partial_\mu J_\mu(\vec{x}) = 0, \tag{68}$$

where $\mu = 0, 1$. When a mass is included in the model, the supercurrent conservation is broken by a term proportional to that mass

$$\partial_\mu J_\mu(\vec{x}) = \frac{m^2}{\lambda} Y(\vec{x}), \tag{69}$$

with

$$Y = N\gamma_i \text{tr}(X_i\Psi), \tag{70}$$

Both the supercurrents J_μ and the breaking term Y are fermionic operators. We can not use the SWTI directly, since the one point function of any fermionic operator vanish

$\langle J \rangle = \langle Y \rangle = 0$. Therefore, we consider the correlation function of the supercurrent with a source operator. For simplicity, we choose $Y_\beta(y)$ as our source operator. Then, the resulting SWTI is

$$\partial_\mu \langle J_{\mu,\alpha}(\vec{x}) Y_\beta(\vec{y}) \rangle = \frac{m^2}{\lambda} \langle Y_\alpha(\vec{x}) Y_\beta(\vec{y}) \rangle - \delta^2(\vec{x} - \vec{y}) \langle Q_\alpha Y_\beta(\vec{y}) \rangle, \tag{71}$$

where Q_α are the supercharges. On the lattice, the Dirac delta function ($\delta^2(\vec{x} - \vec{y})$) tend to spread, thus we expect a better agreement far from the origin where $|\vec{x} - \vec{y}|$ is big. There, we can obtain the effective mass from the ratios

$$\frac{\partial_\mu \langle J_{\mu,\alpha}(\vec{x}) Y_\beta(\vec{y}) \rangle}{\langle Y_\alpha(\vec{x}) Y_\beta(\vec{y}) \rangle} = \frac{m^2}{\lambda}. \tag{72}$$

Therefore, by investigating lattice counterparts of the ratios, we can observe the supersymmetry breaking.

For most of the α β combinations, the correlation function are disappearing ($\partial \langle JY \rangle = \langle YY \rangle = 0$). With the present notation of the gamma matrices (see appendix A.1), only the in cases where $\alpha = \beta$ and $\gamma_{1,\alpha\beta} \neq 0$, the correlation functions are not null. [7] Thus only in those case useful ratios (72) can be obtained. We thus have two set of sixteen ratios, where all the ratios of a set should be equivalent, up to the sign, under the $O(8)$ internal symmetry in the continuum limit.

The lattice supercurrent is prepared using only the forward-type covariant derivative (20). The field strength F_{01} of the supercurrent(67) is obtained with (27). This means that we do not use the lattice counterpart of F_{ij} that includes shift in the fields and backward covariant derivative. We use the naive symmetric difference operator when calculating the divergence of the supercurrent,

$$\partial^s_\mu J_\mu(\vec{x}) = \sum_{\mu=0,1} \frac{J_\mu(\vec{x} + \hat{\mu}) - J_\mu(\vec{x} - \hat{\mu})}{2}. \tag{73}$$

For our computation, we used LAPACK[38] and calculated the inversion of the Dirac operator for all points-to-all points. The correlation functions are averaged over the coordinates to reduce the statistical errors.

3.2.2 Numerical results

To investigate the restoration of SUSY we did simulations with four different physical masses and three different lattice spacings. We used took one configuration every 20 trajectories and used 2000 configurations to obtain our results. The first 6000-10000 trajectories were discarded for thermalization. Table 1 summarizes the simulation parameters.

Figure 10 and 11 show an overview of the $\langle YY \rangle$ term of the SWTI for both the $\alpha = \beta$ and $\gamma_{1,\alpha\beta} \neq 0$ case respectively. We can see a clear signal in both case. In the $\alpha = \beta$,

[7] This is observed numerically and can easily be seen with tree level calculations. It seems to hold at any other of the perturbation theory so even in the strong coupling case this should hold. What is not accounted for are the quantum effect that appear dynamically. Such effect should not appear in our temperature range.

N_t	N_x	m^2/λ	Nconf
12	6	1.00	2000
12	6	0.75	2000
12	6	0.50	2000
12	6	0.25	2000
16	8	1.00	2000
16	8	0.75	2000
16	8	0.50	2000
16	8	0.25	2000
20	10	1.00	2000
20	10	0.75	2000
20	10	0.50	2000
20	10	0.25	2000

Table 1: Simulation parameters and the number of configurations (Nconf) simulated in each case. The dimensionless temperature is $T_{\text{eff}} = 0.3$ and the lattice spacing is determined by $a\lambda^{1/2} = 1/(N_t T_{\text{eff}})$.

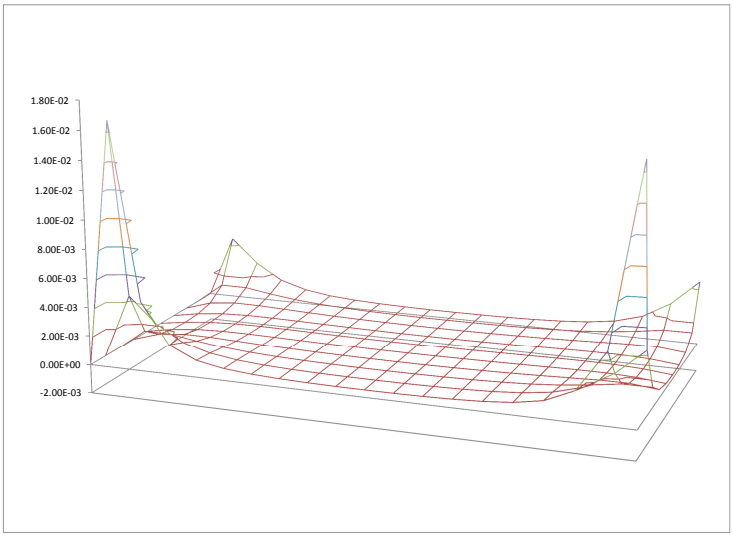

Figure 10: Correlation functions $\langle YY \rangle$ for $\alpha = \beta = 1$. The corresponding parameters are $N_t = 20$, $m^2/\lambda = 0.75$.

the signal is strong far from the origin whereas in the $\gamma_{1,\alpha\beta} \neq 0$ case, because of a sign change, it is small in absolute value. Since this is the region where the influence of the contact term $(\delta^2(\vec{x} - \vec{y}))$ is the weakest, we will get our results from the $\alpha = \beta$ case only. For comparison, a combinations of $(\alpha,\ \beta)$ outside of our studied case is shown in figure 12. In absolute value it is 100 times smaller than our previous case, it is mostly noise within the statistical error. Figure 13 gives a closer look of the shape of the correlation functions.

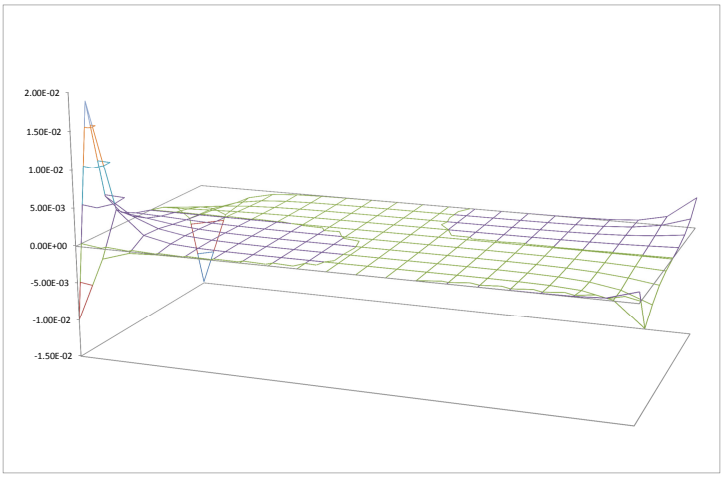

Figure 11: Correlation functions $\langle YY \rangle$ for $\alpha = 1,\ \beta = 10$. The corresponding parameters are $N_t = 20$, $m^2/\lambda = 0.75$. The sign change is the middle of the range makes it difficult to use for the estimation of the SWTI.

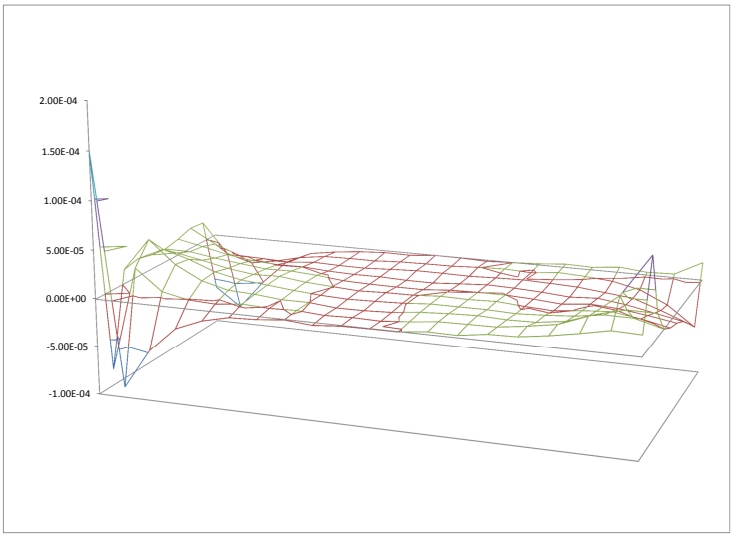

Figure 12: Correlation functions $\langle YY \rangle$ for $\alpha = 1,\ \beta = 2$. The corresponding parameters are $N_t = 20$, $m^2/\lambda = 0.75$. We observe only noise.

To determine to what degree the SWTI holds, we compare the ratios (72) obtained in our simulation with the expected value m^2/λ. Figure 14 shows the ratio for $\alpha = \beta = 1$ with $m^2/\lambda = 0.25$ against t at fixed $x = N_x/2$. We use jackknife analysis to obtain an estimation of the error. The middle of the range of the plot correspond to the point where the supercurrent and source operator are the farthest. In this zone, we have a good

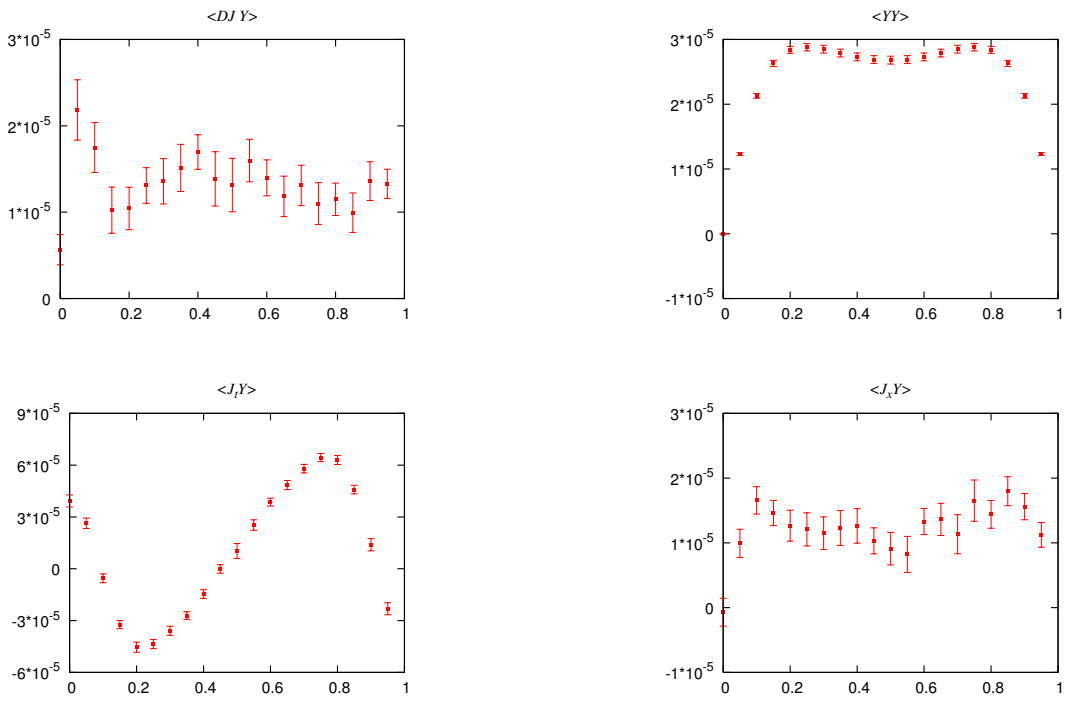

Figure 13: Correlation functions used in our study of the SWTI. The corresponding parameters are $N_t = 20$, $m^2/\lambda = 0.5$. All the correlators are presented as a function of t/N_t at fixed $x = N_x/2$ for $\alpha = \beta = 1$. The other correlators for $\alpha = \beta = 2, \cdots, 16$ behave in the same way.

agreement with the expected value of m^2/λ. Toward the side of the figure ($t = 0, N_t$), the effect of the contact term can be seen in the form of a derivation with the expected value.

The zone far from the contact term is thereafter called the plateau. We estimate the value of the plateau for each $\alpha = \beta$ by performing a constant fit. We use a rectangular zone centered on the point farthest from the origin ($t = N_t/2,\ x = N_x/2$) where the plateau is visible. The area of the plateau is thus somewhat open to interpretation, but the choice of the fit area have an effect smaller than the statistical error on the fit value. Therefore the choice is irreverent to our results.

Table 2 shows the values of the plateau, the fit ranges and χ^2. We find a good agreement between the value of the plateau and m^2/λ. Figure 15 shows the results as a figure. All the values are on a straight line passing through the origin with a slope of one. Thus we can expect that the SUSY hold in some plateau even in the massless limit.

Figure 16 show the result of the continuous limit for all 16 ratios. The continuous limit is taken using a constant fit because of no dependence on the lattice size is observed for the plateau value and linear fit tend to increase the numerical noise badly. The 16 SWTI are visibly equivalent within the statistical error, this shows that we observe the supersymmetry for all 16 supercharges, even if 14 of them are broken by the lattice formulation.

However, these results tell us that the SUSY WTI holds if we ignore the contact term

lattice size	m^2/λ	fit value	χ^2/N_{dof}	fit range
12×6	1.00	1.007 ± 0.043	0.51	3×5
12×6	0.75	0.750 ± 0.029	0.59	3×5
12×6	0.50	0.502 ± 0.013	1.42	5×5
12×6	0.25	0.254 ± 0.006	1.10	5×5
16×8	1.00	0.990 ± 0.044	0.59	5×5
16×8	0.75	0.714 ± 0.029	0.48	5×5
16×8	0.50	0.513 ± 0.015	0.60	5×7
16×8	0.25	0.249 ± 0.005	0.93	7×7
20×10	1.00	1.001 ± 0.043	0.48	9×5
20×10	0.75	0.745 ± 0.026	0.69	9×7
20×10	0.50	0.482 ± 0.012	1.03	11×7
20×10	0.25	0.247 ± 0.005	0.93	11×7

Table 2: Result of the fit of the plateau. The results are averaged over the 16 combinations ($\alpha = \beta$).

lattice size	m^2/λ	N/V
12×6	1.00	$0.50 \pm 0.03\ ^{+0.07}_{-0.06}$
12×6	0.75	$0.49 \pm 0.05\ ^{+0.05}_{-0.03}$
12×6	0.50	$0.49 \pm 0.06\ ^{+0.05}_{-0.06}$
12×6	0.25	$0.47 \pm 0.07\ ^{+0.05}_{-0.06}$
16×8	1.00	$0.57 \pm 0.05\ ^{+0.03}_{-0.06}$
16×8	0.75	$0.56 \pm 0.07\ ^{+0.05}_{-0.04}$
16×8	0.50	$0.56 \pm 0.05\ ^{+0.05}_{-0.05}$
16×8	0.25	$0.53 \pm 0.05\ ^{+0.05}_{-0.04}$
20×10	1.00	$0.64 \pm 0.04\ ^{+0.04}_{-0.05}$
20×10	0.75	$0.65 \pm 0.04\ ^{+0.03}_{-0.03}$
20×10	0.50	$0.65 \pm 0.04\ ^{+0.03}_{-0.02}$
20×10	0.25	$0.63 \pm 0.03\ ^{+0.04}_{-0.03}$

Table 3: $N_\alpha/(L_t L_x)$ for each parameters set. The first and the second column in $N_\alpha/(L_t L_x)$ denote $N_\alpha/(L_t L_x)$ averaged over α and their statistical errors, respectively. While the third column denotes differences among spinors. The upper and lower values in the third column represent the maximum and minimum values of the differences between each $N_\alpha/(L_t L_x)$ and the averages, respectively.

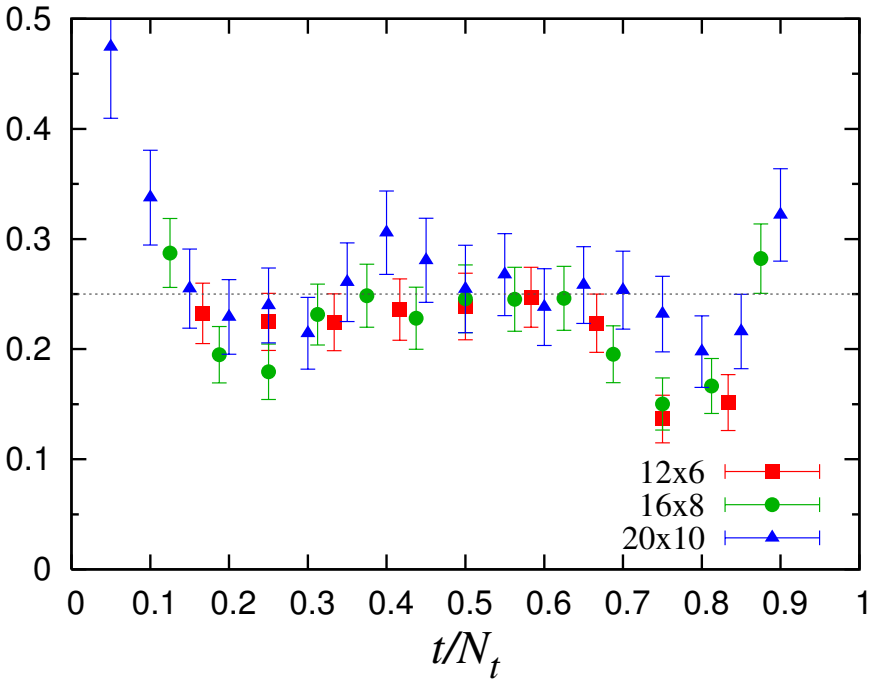

Figure 14: $\frac{\langle \partial_\mu J_{\mu 1}(0) Y_1(t,x)\rangle}{\langle Y_1(0) Y_1(t,x)\rangle}$ as a function of t/N_t at fixed $x = N_x/2$ for $m^2/\lambda = 0.25$ (denoted by the dashed line).

and consider only the plateau region. In the continuum, the SWTI holds everywhere, therefore, in the coutinuum limit of the lattice, the ratios (72) should hold everywhere except at the origin. However on the lattice there is a smearing of the contact term and the SWTI hold only in a smaller area. Thus, to confirm the restoration of the supersymmetry, we need to obserse the reduction of the smearing. By estimating the area of the plateau for different lattice size, we verify that the plateau area tend toward the full area in the continuum limit.

To examine this behavior in a quantifiable way, let us count the numbers of sites on which the ratios are m^2/λ within the errors. We define a subset of the lattice points Γ_α, in which

$$\chi^2_\alpha(\Gamma_\alpha) = \sum_{\vec{x}\in\Gamma_\alpha} \frac{R^2_\alpha(\vec{x})}{(\text{error of } R_\alpha(\vec{x}))^2}, \tag{74}$$

where

$$R_\alpha(\vec{x}) = \frac{\partial_\mu \langle J_{\mu,\alpha}(0) Y_\alpha(\vec{x})\rangle}{\langle Y_\alpha(0) Y_\alpha(\vec{x})\rangle} - \frac{m^2}{\lambda}. \tag{75}$$

Keeping $\chi^2_\alpha(\Gamma_\alpha)/N_\alpha \leq 1$ we took that largest possible Γ_α. This roughly corresponds to the area of the plateau where the SWTI really holds. In the continuous we should have $N_\alpha/(L_t L_x) = 1$. If we do have a restoration of the full symmetry in the continuous limit,

$N_\alpha/(L_t L_x) = 1$ should increase at smaller a. Table 3 shows the $N_\alpha/(L_t L_x)$ ratios. We do observe an increase of the plateau area when approaching to the continuum. This lead to the conclusion that the smearing of the contact term do disappear and the SWTI hold fully in the continuum limit. Moreover, as seen in table 3, the variation of $N_\alpha/(L_t L_x)$ between the spinor is relatively small, the same order than the statistical error. This suggest that all SWTI are degenerated and full SUSY is restored in the continuum limit.

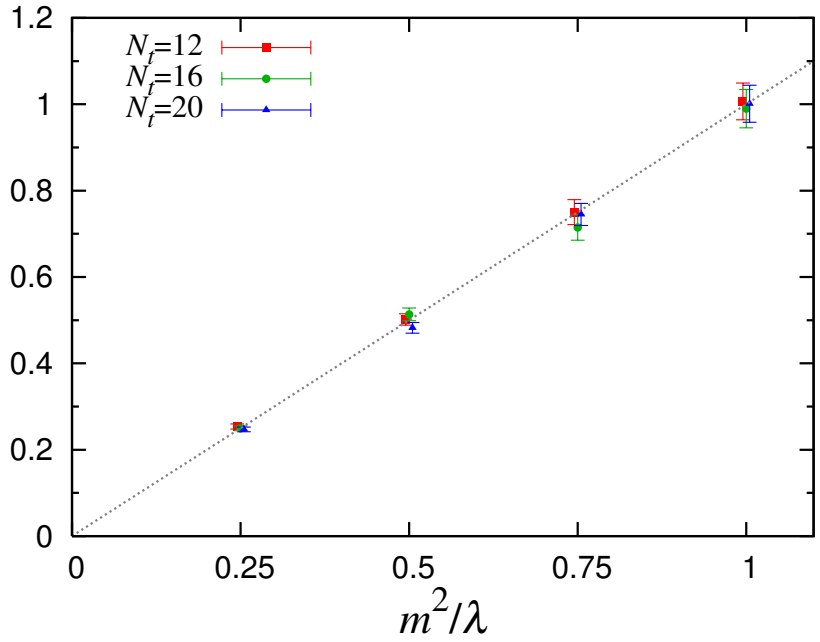

Figure 15: Values of the plateau averaged over $\alpha = \beta$ against the SUSY breaking mass m^2/λ. All the values are on the dashed line passing through the origin with a slope of one.

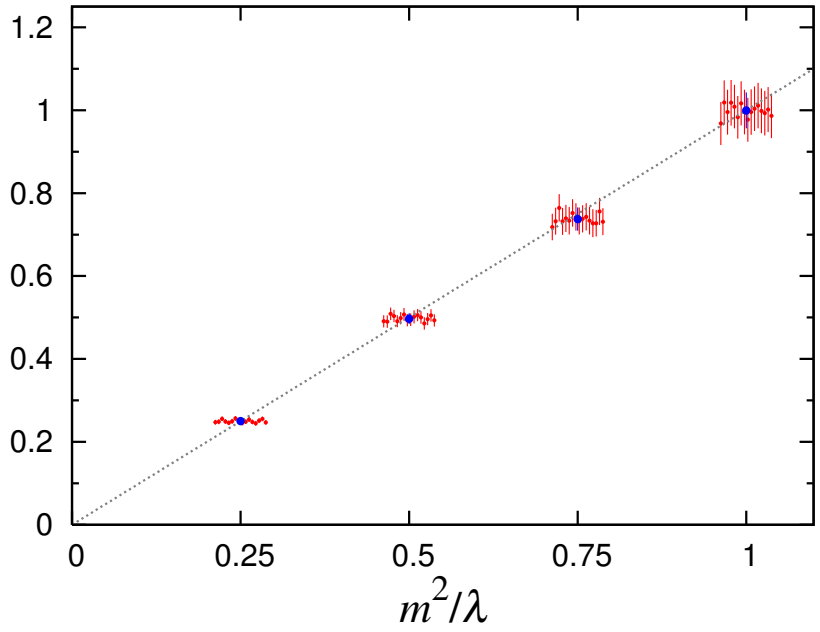

Figure 16: Continuum limit of the values of the plateau obtained for each spinor. The x-axis denotes m^2/λ. The red points with errors separated by a little distance denote the sixteen values corresponding spinors $\alpha = 1, \cdots, 16$ from left to right. The blue points denote the averaged values. The dashed line pass through the origin with a slope of one.

3.3 High temperature expansion

In the high temperature limit, it is possible to study the theory using a perturbation model. In one dimension, such studies were done by Nishimura et al.[41] Here we use their method and applies it to the 2 dimensional case.

We start with the continuum non-twisted action (6) and make a few modifications. First we include the effect of the temperature to the theory by defining the model in a finite volume $L_t \times L_x = \beta \times k\beta$ with $\beta = 1/T$. The boson fields follow periodic boundary conditions as do the fermionic fields in the space direction, in the time direction the fermions are anti-periodic. In this calculation we consider that the action have D boson fields in which d are scalar and p fermions. This cover the theories possessing 4, 8 or 16 supersymmetries.

Model	D	d	p
$\mathcal{N} = (2,2)$ SYM	4	2	4
$\mathcal{N} = (4,4)$ SYM	6	4	8
$\mathcal{N} = (8,8)$ SYM	10	8	16

The first step in the calculation is to add a gauge fixing terms in the form

$$S_{gf} = \frac{N}{2\lambda}\int_0^\beta \mathrm{d}t \int_0^{k\beta} \mathrm{d}x \ \mathrm{tr}\Big\{\frac{(\partial_\mu X_\mu)^2}{\xi} + \partial_\mu \bar{c} D_\mu c\Big\}. \tag{76}$$

The fields $\bar{c}$ and c are the Faddeev-Popov ghosts. The gauge fixing parameter ξ is set to 1 thereafter for simplicity. The action with this fixing term included is

$$\begin{aligned} S = \frac{N}{2\lambda}\int_0^\beta \mathrm{d}t \int_0^{k\beta} \mathrm{d}x \ \mathrm{tr}\Big\{&(\partial_\mu X_a)^2 + 2i\partial_\mu X_a[X_\mu, X_a] - \frac{1}{2}[X_a, X_b]^2 \\ &+ \Psi\partial_0\Psi - i\Psi\gamma_1\partial_1\Psi + \Psi\gamma_a[X_a, \Psi] \\ &+ \partial_\mu\bar{c}\partial_\mu c + i\partial_\mu\bar{c}[X_\mu, c]\Big\}. \end{aligned} \tag{77}$$

Here μ is running from 0 to 1 and a, b from 0 to $d+1$.

We do a Fourier transformation of the action then renormalize the fields in order to make the temperature contribution evident. The Fourier transformations of the fields are

$$X_a(t,x) = \sum_{(n_t,n_x)\in\mathbb{Z}} \tilde{X}_a(n_t,n_x) e^{i\frac{2\pi}{\beta}n_t t + i\frac{2\pi}{k\beta}n_x x}, \tag{78}$$

$$\Psi(t,x)_\alpha = \sum_{(n_t,n_x)\in\mathbb{Z}} \tilde{\Psi}_\alpha(n_t+\tfrac{1}{2},n_x) e^{i\frac{2\pi}{\beta}(n_t+\frac{1}{2})t + i\frac{2\pi}{k\beta}n_x x}, \tag{79}$$

$$c(t,x) = \sum_{(n_t,n_x)\in\mathbb{Z}} \tilde{c}(n_t,n_x) e^{i\frac{2\pi}{\beta}n_t t + i\frac{2\pi}{k\beta}n_x x}, \tag{80}$$

$$\bar{c}(t,x) = \sum_{(n_t,n_x)\in\mathbb{Z}} \tilde{\bar{c}}(n_t,n_x) e^{-i\frac{2\pi}{\beta}n_t t - i\frac{2\pi}{k\beta}n_x x}. \tag{81}$$

The rescaling is done in order to make the fields unitless and bring their strongest term

to the order of one. Here we rescale the fields considering k to be of the order one

$$\lambda^{1/4}\beta^{-1/2}k^{1/4}\hat{A}_a = \tilde{X}_a(0,0), \tag{82}$$

$$\lambda^{1/2}\hat{X}_a(n_t,n_x) = \tilde{X}_a(n_t,n_x), \qquad (n_t,n_x)\neq(0,0) \tag{83}$$

$$\lambda^{1/2}\beta^{-1/2}\hat{\Psi}_\alpha(n_t+\tfrac{1}{2},n_x) = \tilde{\Psi}_\alpha(n_t+\tfrac{1}{2},n_x), \tag{84}$$

$$\lambda^{1/2}\hat{c}(n_t,n_x) = \tilde{c}(n_t,n_x), \tag{85}$$

$$\lambda^{1/2}\hat{\bar{c}}(n_t,n_x) = \tilde{\bar{c}}(n_t,n_x). \tag{86}$$

Here we consider that the field $\bar{c},c$ do not have a zero mode. Also we use the gauge group $U(N)$. The $U(1)$ contribution can easily removed to obtain the $SU(N)$ models. The boson zero modes $\hat{A}_a$ do not have the $U(1)$ since these modes do not contribute to the action in any way. After the rescaling, the action can then be written in power of the parameter $\gamma = \lambda^{1/4}\beta^{1/2}$, which is small at high temperature, therefore used as our expansion parameter. The action become

$$S = S_{kin} + S_0 + S_{int}. \tag{87}$$

The two first terms are of the order one and constitute the main part of the action

$$\begin{aligned} S_{kin} = \sum_{n_t,n_x}\mathrm{tr}\Big\{ & 2\pi^2 N\Big(kn_t^2+\frac{n_x^2}{k}\Big)\hat{X}_a(n_t,n_x)\hat{X}_a(-n_t,-n_x) \\ & +\pi N\hat{\Psi}(-n_t-\tfrac{1}{2},-n_x)_\alpha(ik(n_t+\tfrac{1}{2})\delta_{\alpha\beta}+n_x(\gamma_1)_{\alpha\beta})\hat{\Psi}(n_t+\tfrac{1}{2},n_x)_\beta \\ & +2\pi^2 N\Big(kn_t^2+\frac{n_x^2}{k}\Big)\hat{\bar{c}}(n_t,n_x)\hat{c}(n_t,n_x)\Big\}, \end{aligned} \tag{88}$$

$$S_0 = -\frac{N}{4}\mathrm{tr}[\hat{A}_a,\hat{A}_b][\hat{A}_a,\hat{A}_b]. \tag{89}$$

The last term is a perturbation

$$S_{int} = \gamma S_1 + \gamma^2 S_2 + \gamma^3 S_3 + \gamma^4 S_4, \tag{90}$$

with

$$\begin{aligned} S_1 = \sum_{n_t,n_x}\mathrm{tr}\Big\{ & -2N\pi k^{3/4}n_t\hat{X}_a(n_t,n_x)[\hat{A}_0,\hat{X}_a] - 2N\pi k^{-1/4}n_x\hat{X}_a(n_t,n_x)[\hat{A}_1,\hat{X}_a] \\ & -2N\pi k^{3/4}n_t\hat{X}_a(n_t,n_x)[\hat{X}_0,\hat{A}_a] - 2N\pi k^{-1/4}n_x\hat{X}_a(n_t,n_x)[\hat{X}_1,\hat{A}_a] \\ & +\frac{Nk^{3/4}}{2}\hat{\Psi}\gamma_a[\hat{A}_a,\hat{\Psi}] - N\pi k^{3/4}n_t\hat{\bar{c}}(n_t,n_x)[\hat{A}_0,\hat{c}] - N\pi k^{-1/4}n_x\hat{\bar{c}}(n_t,n_x)[\hat{A}_1,\hat{c}]\Big\}, \end{aligned} \tag{91}$$

$$\begin{aligned} S_2 = \sum_{n_t,n_x}\mathrm{tr}\Big\{ & -2N\pi k n_t\hat{X}_a(n_t,n_x)[\hat{X}_0,\hat{X}_a] - 2N\pi n_x\hat{X}_a(n_t,n_x)[\hat{X}_1,\hat{X}_a] \\ & +\frac{kN}{2}\hat{\Psi}\gamma_a[\hat{X}_a,\hat{\Psi}] - N\pi k n_t\hat{\bar{c}}(n_t,n_x)[\hat{X}_0,\hat{c}] - N\pi n_x\hat{\bar{c}}(n_t,n_x)[\hat{X}_1,\hat{c}] \\ & -\frac{k^{1/2}N}{2}[\hat{X}_a,\hat{A}_b][\hat{X}_a,\hat{A}_b] - \frac{k^{1/2}N}{2}[\hat{A}_a,\hat{A}_b][\hat{X}_a,\hat{X}_b] - \frac{k^{1/2}N}{2}[\hat{X}_a,\hat{A}_b][\hat{A}_a,\hat{X}_b]\Big\}, \end{aligned} \tag{92}$$

$$S_3 = \sum_{n_t,n_x} \mathrm{tr}\Big\{ - k^{3/4} N [\hat{X}_a, \hat{X}_b][\hat{X}_a, \hat{A}_b]\Big\}, \tag{93}$$

$$S_4 = \sum_{n_t,n_x} \mathrm{tr}\Big\{ - \frac{kN}{4} [\hat{X}_a, \hat{X}_b][\hat{X}_a, \hat{X}_b]\Big\}. \tag{94}$$

The momentum conservation is implicit.

This allows us to calculate an observable using the following relations

$$\langle O \rangle = \frac{\langle \sum_{n=0}^{\infty} \frac{1}{n!} \langle\langle O(-S_{int})^n \rangle\rangle \ \rangle_0}{\langle \sum_{n=0}^{\infty} \frac{1}{n!} \langle\langle (-S_{int})^n \rangle\rangle \ \rangle_0}. \tag{95}$$

The kinetic part of the correlation function

$$\langle\langle O \rangle\rangle = \frac{\int D\hat{X} D\hat{\bar{c}} D\hat{c} D\hat{\Psi} O e^{-S_{kin}}}{\int D\hat{X} D\hat{\bar{c}} D\hat{c} D\hat{\Psi} e^{-S_{kin}}} \tag{96}$$

can be calculated analytically. The propagators are

$$\langle\langle \hat{X}_a^{ij}(\vec{n}) \hat{X}_b^{kl}(\vec{m}) \rangle\rangle = \frac{\delta_{ab}\delta_{il}\delta_{jk}\delta_{\vec{n}+\vec{m}}}{(2\pi)^2 N (k n_t^2 + N_x^2/k)}, \tag{97}$$

$$\langle\langle \hat{\bar{c}}^{ij}(\vec{n}) \hat{c}^{kl}(\vec{m}) \rangle\rangle = \frac{-\delta_{il}\delta_{jk}\delta_{\vec{n}-\vec{m}}}{(2\pi)^2 N (k n_t^2 + N_x^2/k)}, \tag{98}$$

$$\langle\langle \hat{\Psi}_\alpha^{ij}(\vec{n}) \hat{\Psi}_\beta^{kl}(\vec{m}) \rangle\rangle = \frac{(ik(n_t+1/2)\delta_{\alpha\beta} - n_x \gamma_{1,\alpha\beta})\delta_{il}\delta_{jk}\delta_{\vec{n}+\vec{m}}}{(2\pi) N (k^2(n_t+1/2)^2 + n_x^2)}. \tag{99}$$

The other sub-correlation function that we use is

$$\langle O \rangle_0 = \frac{\int D\hat{A} O e^{-S_0}}{\int D\hat{A} e^{-S_0}}. \tag{100}$$

This corresponds to the boson zero-modes. It takes the form of a matrix model and is approximated using numerical simulations. The used observables from this part are

$$\theta_1 = \langle \frac{1}{N} \mathrm{tr}(\hat{A}_a^2) \rangle_0, \tag{101}$$

$$\theta_2 = \langle \mathrm{tr}(\hat{A}_a^2) \mathrm{tr}(\hat{A}_a^2) \rangle_0, \tag{102}$$

$$\theta_3 = \langle \mathrm{tr}(\hat{A}_a^2) \mathrm{tr}(\hat{A}_b^2) \rangle_0, \tag{103}$$

$$\theta_4 = \Big\langle \sum_{a,b} \frac{1}{N} \mathrm{tr}(-[\hat{A}_a, \hat{A}_b]^2) tr(\hat{A}_c^2) \Big\rangle_0, \tag{104}$$

$$\theta_5 = \langle \frac{1}{N} \mathrm{tr}(\hat{A}_a^4) \rangle_0, \tag{105}$$

$$\theta_6 = \langle -\frac{N}{4} \mathrm{tr}[\hat{A}_a, \hat{A}_b][\hat{A}_a, \hat{A}_b] \rangle_0. \tag{106}$$

Here, there is no summation over the indices if not explicitly indicated, also different indices can not be equal ($a \neq b$). The results of this simulation have been calculated by

Nishimura et al.[41] and can be found in the appendix A.2. Thus the leading part of any observable is calculated with

$$\langle O\rangle \approx \langle\ \langle\langle O\rangle\rangle\ \rangle_0, \tag{107}$$

and the following terms in the perturbation are

$$\begin{aligned}\langle O\rangle_{O(\gamma^2)} =& -\gamma\langle\ \langle\langle OS_1\rangle\rangle\ \rangle_0 + \gamma^2\langle\ \langle\langle O(\tfrac{1}{2}S_1^2 - S_2)\rangle\rangle\ \rangle_0 \\ &-\gamma^2\langle\ \langle\langle O\rangle\rangle\ \rangle_0\langle\ \langle\langle(\tfrac{1}{2}S_1^2 - S_2)\rangle\rangle\ \rangle_0 \\ =&\gamma\langle OS_1\rangle_c + \gamma^2\langle O(\tfrac{1}{2}S_1^2 - S_2)\rangle_c\end{aligned} \tag{108}$$

where $\langle O\rangle_c$ is the connected part of $\langle\ \langle\langle O\rangle\rangle\ \rangle_0$. We keep term up to the order of γ^2 because for most observables, it is the next to leading order contribution. The terms proportional to γ are forbidden by symmetry.

We first calculate the scale of the scalar fields

$$R^2 = \frac{\gamma^2}{N\beta^2}\mathrm{tr}(A_i^2) + \sum_{\vec{n}\neq 0}\frac{\gamma^4}{N\beta^2}\mathrm{tr}(X_i^2). \tag{109}$$

The leading term is given by

$$\frac{\gamma^2}{N\beta^2}\langle\mathrm{tr}(A_i^2)\rangle_0 = \frac{\gamma^2}{\beta^2}d\theta_1 \tag{110}$$

This only includes the bosonic zero-mode effect, the fermion contribution and the non-zero mode effect appears in the next-to-leading order. The kinetic part needs only to be calculated to the first order

$$\frac{\gamma^4}{N\beta^2}\langle\mathrm{tr}(X_i^2)\rangle_= \frac{\gamma^4}{\beta^2}d\sigma \tag{111}$$

The zero-mode with the first non disappearing perturbation term is

$$\frac{\gamma^2}{N\beta^2}\langle\mathrm{tr}(A_i^2)(\tfrac{1}{2}S_1^2 - S_2)\rangle_c = \frac{\gamma^4 k}{\beta^2}(\theta_2 + (d-1)\theta_3)(pd/2\sigma_{1/2} - d^2\sigma). \tag{112}$$

where the σ corresponds to the summation over the modes.

$$\sigma = \sum_{\vec{n}\neq 0}\frac{1}{(2\pi)^2(kn_t^2 + n_x^2/k)}, \tag{113}$$

$$\sigma_{1/2} = \sum_{\vec{n}}\frac{1}{(2\pi)^2(k(n_t+1/2)^2 + n_x^2/k)}. \tag{114}$$

Both $\sigma_{1/2}$ and σ are divergent, however the difference $(\sigma_{1/2} - \sigma)$ is finite. For the various 2D super Yang-Mills models, we have $(d,p) = (2,4),(4,8),(8,16)$, therefore $pd/2 = d^2$ in every cases. Many divergences are canceled this way. The value of the summation is in table 4 in appendix A.2. The resulting scalar magnitude is

$$\langle R^2\rangle \approx \frac{\gamma^2}{\beta^2}d\theta_1 + \frac{\gamma^4}{\beta^2}d\sigma + \frac{\gamma^4 k}{\beta^2}d^2(\theta_2 + (d-1)\theta_3)(\sigma_{1/2} - \sigma) + O(\gamma^6/\beta^2) \tag{115}$$

This value diverges, there is a σ factor that is not canceled. This was to be expected since this observable is not invariant under supersymmetry. The cancellation of the divergences present in the model are mostly based on supersymmetry. Moreover R^2 is written using both γ and β, this is to represent the units of R^2. γ is unitless whereas β has a mass dimension of -1.

Next, we will be interested in the value of the action. As will be shown later in 4.1, the action can be connected to the internal energy and pressure of the model. The action is decomposed in power of γ, and up to the next to leading order we have

$$\langle S\rangle = \langle\ \langle\langle S_{kin}\rangle\rangle\ \rangle_0 + \langle\ \langle\langle S_0\rangle\rangle\ \rangle_0 + \langle\ \langle\langle S_H\rangle\rangle\ \rangle_0 \tag{116}$$

$$+\gamma^2(\langle\ \langle\langle S_2\rangle\rangle\ \rangle_0 - \langle S_1^2\rangle_c + \langle (S_{kin}+S_0)(\tfrac{1}{2}S_1^2 - S_2)\rangle_c) + O(\gamma^4) \tag{117}$$

where the S_H is the auxiliary field part of the action. There are $d-1$ auxiliary fields. The leading order is given by

$$\langle S\rangle = N^2\bigg(-\sum_H \frac{p}{2} + \sum_I \frac{(d+1)+(d-1)}{2} + \frac{(d-1)}{2}\bigg) + \theta_6. \tag{118}$$

Here in the first term we have a sum over the fermion modes $\sum_H$, which corresponds to a sum over the mode with a half-integer time direction momentum and integer space momentum. The $\sum_I$ represent the sum over bosonic mode represented by integer momentum in both directions and with the zero mode removed. Both summations diverge in the continuum theory and to resolve the divergence we put a cut-off to the summation. When the summation is done inside a L_t per L_x periodic box, like one that would be obtained if space was discretized in a lattice, the summations always result in one extra mode for the fermion. This corresponds to the lacking zero-mode in the boson mode summation. The boson zero mode can also be done analytically, the θ_6 correspond to the gauge and scalar bosons zero part. The auxiliary fields zero modes give an extra $N^2(d-1)/2$ contribution. The resulting leading order of the action is

$$\langle S\rangle = (N^2-1)\frac{d+2}{4} - N^2\frac{d+1}{2}. \tag{119}$$

The next to leading order(NLO) term is given by

$$\langle S\rangle_{NLO} = -\frac{\gamma^2 N^2 d^2}{4k^{1/2}}\theta_4(\sigma_{1/2}-\sigma). \tag{120}$$

As expected, this value, being supersymmetric, do not diverge.

Figure 17 shows the measured value of the action at high temperature with the expected results from the high temperature expansion. We see that the action tends toward the leading order expectation at high temperature. In the highest temperature range the data fit with the calculation up to the NLO. However, there are big statistical errors and no simulations were performed at higher temperature, the data appears imperfect.

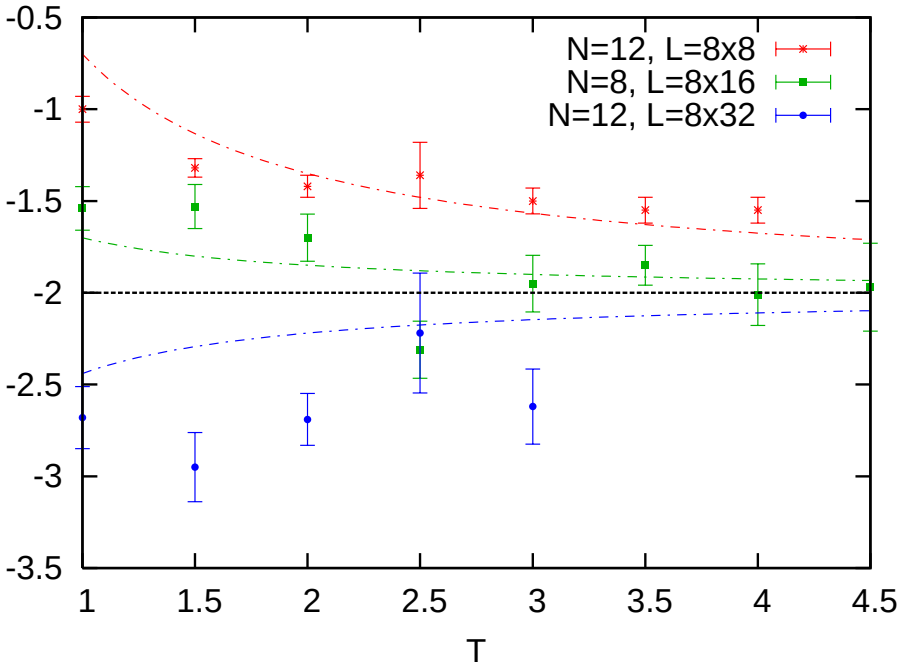

Figure 17: Expectation value of the action as a function of the temperature. The black dotted line is the first order calculation. The dashed lines are the high temperature expansion up to the NLO. At high temperature ($T > 3$) the data fit relatively well.

Next we calculate the Polyakov lines. The Polyakov lines are given by

$$\begin{aligned}\langle P_0\rangle &= \frac{1}{N}\mathrm{tr}\langle Pexp\big(i\int_0^\beta dtX_0(t,x)\big)\rangle \\ &\approx 1-\frac{\gamma^2}{2Nk^{1/2}}\langle \mathrm{tr}\hat{A}_0^2\rangle + \frac{\gamma^4}{4!Nk}\langle \mathrm{tr}\hat{A}_0^4\rangle + O(\gamma^6), \qquad (121)\\ \langle P_1\rangle &= \frac{1}{N}\mathrm{tr}\langle Pexp\big(i\int_0^{k\beta} dtX_1(t,x)\big)\rangle \\ &\approx 1-\frac{\gamma^2 k^{3/2}}{2N}\langle \mathrm{tr}\hat{A}_1^2\rangle + \frac{\gamma^4 k^3}{4!N}\langle \mathrm{tr}\hat{A}_1^4\rangle + O(\gamma^6). \qquad (122)\end{aligned}$$

Up to the next to leading order, the Polyakov lines can be determined using the zero mode only. For the spacial line, the expansion parameter is not γ^2 but $\gamma^2 k^{3/2}$, this means that at high k this expansion is invalid. In this case, the Polyakov line takes a value around 0, not around 1. The resulting expansion is

$$\langle P_0\rangle = 1-\frac{\gamma^2}{2k^{1/2}}\theta_1 - \frac{\gamma^4 d}{2}\big(\sigma_d(\theta_3-\theta_2)+d(\sigma_{1/2}-\sigma)\theta_3\big)+\frac{\gamma^4}{24k}\theta_6, \qquad (123)$$

$$\langle P_1\rangle = 1-\frac{k^{3/2}\gamma^2}{2}\theta_1 - \frac{\gamma^4 k^2 d}{2}\big(\sigma_d(\theta_3-\theta_2)+d(\sigma_{1/2}-\sigma)\theta_3\big)+\frac{\gamma^4 k^3}{24}\theta_6, \qquad (124)$$

with

$$\sigma_d = \sum_{\vec{n}} \frac{(k(n_t+1/2)^2 - n_x^2/k)}{(2\pi)^2(k(n_t+1/2)^2 + n_x^2/k)^2} - \sum_{\vec{n}\neq 0} \frac{(kn_t^2 - n_x^2/k)}{(2\pi)^2(kn_t^2 + n_x^2/k)^2}. \tag{125}$$

The summation is tabulated in appendix A.2.

Figure 18 shows the measured value of the temporal Polyakov line (P_t) at high temperature with the expected results from the high temperature expansion up to the NLO. Only at high temperature ($T > 4$), the simulations results seem to fit the expectations. At low temperature the NLO term dominates the leading order term, predicting value over one, which outside the range of the Polyakov line. Unless higher temperature simulations are made it is difficult to confirm agreement with the high temperature expansion results.

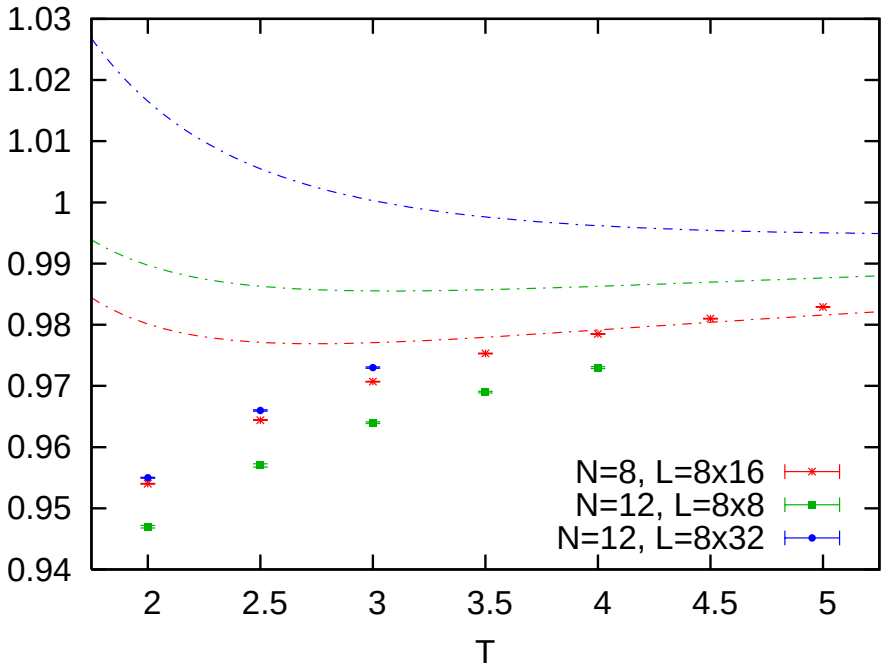

Figure 18: Expectation value of the temporal Polyakov line as a function of the temperature. The dashed lines are the high temperature expansion up to the NLO. At high temperature ($T > 4$) the data is consistent with the expansion.

From our simulation results at high temperature, we can say that our simulations are giving results consistent with the perturbative calculations. However, due to the lack of very high temperature simulations and the large statistical error, we cannot confirm the validity of the lattice simulations using the perturbative calculations.

4 Duality

4.1 Choice of physical quantity

To test the gauge-gravity duality, we need to observe a physical quantity that can be obtained both with the lattice simulations of the gauge theory and the black p-brane calculations. In the gravity side, we can calculate the black-hole thermodynamics, therefore we have access to the energy and entropy and related quantities. In the gauge side, the equation of the energy is also simple to obtain either using a Legendre transformation or the partition function. The partition function is related to the Hamiltonian by

$$Z = \int D\Psi DADX e^{-S(A,X,\Psi)} = e^{-\beta H}. \tag{126}$$

Therefore the energy can be obtained by

$$\begin{aligned} \langle E \rangle &= -\frac{\partial}{\partial \beta} ln(Z) \\ &= \frac{1}{Z} \int D\varphi \frac{\partial S}{\partial \beta} e^{-S}. \end{aligned} \tag{127}$$

Here the measure $(D\varphi)$ is considered independent of β.

The continuum not-twisted action of the gauge theory (6) at finite temperature is

$$\begin{aligned} S = \frac{N}{\lambda} \int_0^\beta \mathrm{d}t \int_0^L \mathrm{d}x \ \mathrm{tr} \Big\{ &\frac{1}{4} F_{\mu\nu}^2 + \frac{1}{2} (D_\mu X_i)^2 - \frac{1}{4} [X_i, X_j]^2 \\ &+ \frac{1}{2} \Psi_\alpha D_0 \Psi_\alpha - \frac{i}{2} \Psi_\alpha (\gamma_1)_{\alpha\beta} D_1 \Psi_\beta + \frac{1}{2} \Psi_\alpha (\gamma_i)_{\alpha\beta} [X_i, \Psi_\beta] \Big\}. \end{aligned} \tag{128}$$

The field are dependent on β in their (anti-)periodicity $\varphi(t+\beta, x) = \pm\varphi(t, x)$. In order to isolate the dependence, we rescale the fields by

$$A_\mu = A'_\mu \beta^{-1} \quad X_i = X'_i \beta^{-1} \quad \Psi_\alpha = \Psi'_\alpha \beta^{-1.5} \tag{129}$$

$$d_0 = d'_0 \beta^{-1} \quad \mathrm{d}t = \mathrm{d}t' \beta. \tag{130}$$

This choice comes from the unit of the fields, the renormalization makes the fields unitless. It does not affect the measure of the integral because of the supersymmetry. When the seven auxiliary fields (H) are included the measure becomes $DADXD\Psi DH = (\beta^{-1\cdot 2} DA)(\beta^{-1\cdot 8} DX)(\beta^{1.5\cdot 16} D\Psi)(\beta^{-2\cdot 7} DH)$. This cancellation also arise in other SYM model. Now applying the derivative we get

$$\langle E \rangle = \frac{-3}{\beta} \langle S \rangle + \frac{1}{\beta} \langle \Delta \rangle. \tag{131}$$

with

$$\begin{aligned} \Delta =& \frac{N}{\lambda} \int_0^\beta \mathrm{d}t \int_0^L \mathrm{d}x d_1 A_0 F_{01} + d_1 X_i D_1 X_i - \frac{i}{2} \Psi_\alpha (\gamma_1)_{\alpha\beta} d_1 \Psi_\beta \\ =& \frac{N}{16\lambda} \int_0^\beta \mathrm{d}t \int_0^L \mathrm{d}x Q_\alpha \mathrm{tr} \ (\gamma_1 \gamma_a)_{\alpha\beta} \Psi_\beta d_1 X_a \end{aligned} \tag{132}$$

This expression is a supersymmetric invariant quantity, thus the zero of the energy is well defined. A different, but equally valid, expression can be obtained from a Legendre transformation.

However, this quantity is somewhat problematic when understood as a lattice quantity. Part of the problem is of computational nature, the fermions 2-points functions in Δ are costly numeriacally to obtain with simulations, making it hard to obtain a lot of configurations.[8] Also, the fermions two points functions are also associated with big statistical error, as a results a good amount of configuration is needed to get satisfying results. Lastly, while the Δ is Q-exact in the continuous model, it is not on the lattice since all 16 supercharges are needed. This means that the zero-point energy is not well defined on the lattice. Having observed that the full supersymmetry is restored in the continuum limits, it would be possible to measure the energy as a function of the lattice spacing $E(T, a)$, then taking the continuum limit. This would also increase the amount of calculations and the statistical error on the final results. Therefore using the energy is slow and coslty, and we avoided it.

To get a practical quantity on the lattice, we can redo the calculation using the lattice definition of β. The lattice sizes are

$$\beta = aN_t \quad L = aN_x \tag{133}$$

with a being the lattice spacing. If we change the derivative in 127 for

$$\frac{\partial}{\partial\beta} \to \frac{1}{N_t}\frac{\partial}{\partial a}. \tag{134}$$

Then, using the same procedure as before, renormalizing by a this time then applying the derivative, we get

$$\frac{1}{N_t}\frac{\partial S}{\partial a} = \frac{-2}{\beta}S. \tag{135}$$

This is easily obtained with lattice simulation. The fermionic part of the action can be analytically calculated and the bosonic part is already calculated at every trajectory. However, this quantity is not the energy since the lattice spacing apply both to the time and space directions. We have

$$\frac{-1}{N_t}\frac{\partial}{\partial a}ln(Z(\beta, L)) = \frac{-1}{N_t}\frac{\partial\beta}{\partial a}\frac{\partial}{\partial\beta}ln(Z(\beta, L)) - \frac{1}{N_t}\frac{\partial L}{\partial a}\frac{\partial}{\partial L}ln(Z(\beta, L)) \tag{136}$$

$$= \langle E\rangle - L\langle P\rangle. \tag{137}$$

P is the pressure. As will be shown in the next section, this quantity can be evaluated from the thermodynamics of the black-hole. We therefore choose

$$Z \equiv E - PL \tag{138}$$

as the physical quantity that we use to observe the duality.

[8]The computation of an inverse matrix scale to the third power of the size of the matrix, thus to the sixth power of the gauge group $\propto N^6$. A computation that took 20 min in SU(2) (calculation of SWTI with a lattice size of $N_t = 16,\ N_x = 8$) will take over 650 days for SU(6), if calculated directly. The main problem being the matrix inversion calculations cannot be efficiently run in parallel computations. Approximative methods, which allow for parallelization, can bring the computation time to a reasonable amount.

4.2 Black p-brane thermodynamics

In this section, we calculate $E-PL$ in the gravity side of the duality. The two dimensional SYM model correspond to a D1-brane in the gravity side[4], whose classical solution is an extremal black p-brane. The supergravity metric associated with black p-brane similar to a black-hole metric with electric charge, therefore it is a simple task to apply black hole thermodynamics to it. The extremal black 1-brane entropy disappear, thus we look at the near extremal case for the thermodynamics.

The supergravity action with a black 1-brane as it's source is given by[40],

$$S = -\frac{1}{2\kappa^2}\int d^{10}x\sqrt{g}[R - \frac{1}{2}(\partial\phi)^2 - \frac{1}{2\ 7!}e^{\phi}F_7^2]. \tag{139}$$

Here κ corresponds to the gravitational constant, g is the metric and R the space curvature. ϕ is the dilation field and F_7 is the field strength for a purely magnetic solution. Whether we use a magnetic or dyonic charge does not affect the metric and therefore the associated black-hole thermodynamics.

From the equations of motion of the action, the metric can be obtained. In Einstein frame, we have

$$ds^2 = H^{1/4}(r)\bigg(H^{-1}(r)[f(r)dt^2 + dx^2] + f^{-1}(r)dr^2 + r^2 d\Omega_7^2\bigg) \tag{140}$$

with

$$H(r) = 1 + \sinh^2\gamma\frac{r_0^6}{r^6} \tag{141}$$

$$f(r) = 1 - \frac{r_0^6}{r^6}. \tag{142}$$

r_0 is the radius of the horizon. In the extremal limit, this solution correspond to the classical solutions of a D1-brane. The near-extremal limit is obtained by taking $r_0 \to 0$, $\gamma \to \infty$ while keeping $\sinh 2\gamma r_0^6$ fixed. The classical solution is a good approximation of the full physics of the D-brane when the black-hole radius is large compared to the string lenght α'. This is fullfilled at large N and large coupling or low temperature. The black string is considered periodic with a period L.

The charge density is given by

$$q = \frac{3\omega_7}{\sqrt{2}\kappa}r_0^6\sinh 2\gamma \tag{143}$$

and keep constant when taking the near-extremal limit. It is obtained from the equation of motion of the gauge field in the supergravity action.

The thermodynamics are directly obtained form the metric. From the surface gravity

$$g_{surf} = \frac{1}{2}\sqrt{\left(\frac{\partial}{\partial r}(-g_{tt})\right)(r_0)\left(\frac{\partial}{\partial r}g_{rr}\right)(r_0)}, \tag{144}$$

we obtain the temperature of the black string

$$T = \frac{g_{surf}}{2\pi,} \tag{145}$$

$$= \frac{3}{2\pi r_0} H^{-1/2}(r_0), \tag{146}$$

$$\propto \frac{r_0^2}{\sqrt{q}} \quad (\gamma \to \infty) \tag{147}$$

We observe, from the last line, extremal black-hole is null.

The Bekenstein-Hawking entropy is proportional to area of the black hole

$$A = \omega_7 L g_{xx}^{1/2}(r_0) g_{\Omega\Omega}^{7/2} \tag{148}$$

which gives

$$S = \frac{2\pi A}{\kappa^2}, \tag{149}$$

$$= \frac{2\pi}{\kappa^2} \omega_7 L r_0^7 H^{1/2}(r_0), \tag{150}$$

$$\propto L r_0^4 \sqrt{q}. \quad (\gamma \to \infty) \tag{151}$$

The entropy disappear in the extremal limit. The entropy is better expressed as a function of the temperature, for the near-extremal limit

$$S = \frac{(2\pi)^3}{9\kappa^2} \omega_7 q^{3/2} L T^2. \tag{152}$$

Lastly, the internal energy of the black-brane is calculated using the first law of thermodynamics $dE = TdS$. The energy is

$$E = \frac{2}{3} \frac{(2\pi)^3}{9\kappa^2} \omega_7 q^{3/2} L T^3 \tag{153}$$

up to a constant which we set to zero for our purpose.

We must now give a value to the charge of the brane q and to the gravitational constant κ. The charge, gravitational constant and yang-mills coupling constant in string unit for a D1-string are given by

$$2\kappa^2 = (2\pi)^7 \alpha'^4 g_s, \tag{154}$$

$$q = N(2\pi)^{5/2} \alpha', \tag{155}$$

$$g_{YM} = \frac{N^{1/2}}{\lambda^{1/2}} = \frac{2\pi\alpha'}{g_s}, \tag{156}$$

where N is the gauge group size, α' the string length and g_s the string coupling constant. The definition of the gravitational constant in string unit (154) is calculated from graviton scattering calculations. The charge density (155) is proportional to the number of D-brane. By comparing the gauge sector of the string action with a gauge action, the

Yang-Mills coupling ($g^2_{YM} = \lambda/N$) can be written in string units. The resulting energy and entropy are

$$e(t) = \frac{2C_1}{3} l N^2 t^3, \tag{157}$$

$$S(t) = C_1 l N^2 t^2. \tag{158}$$

where

$$C_1 = \frac{2^4 \pi^{5/2}}{3^3} \approx 10.37 \tag{159}$$

e, l and t are the unitless energy, brane length and temperature respectively.

$$e = \frac{E}{\sqrt{\lambda}} \quad l = \sqrt{\lambda} L \quad t = \frac{T}{\sqrt{\lambda}} \tag{160}$$

From the internal energy, we derive the free energy ($F = E - TS$) and pressure. The equivalent of the space volume is the string length. The pressure is

$$-p = -\frac{P}{\lambda} = \frac{\partial(e - tS)}{\partial l} = (-1/3) C_1 N^2 T^3. \tag{161}$$

Therefore the desired physical quantity is

$$e - pl = (1/3) C_1 N^2 l t^3 \approx 3.46 N^2 l t^3. \tag{162}$$

We will compare this value with the results of our simulation in the next section.

4.3 Observation of Gauge-Gravity Duality

The simulations computed in order to observe the duality were done with a reasonably large group of $N = 12$. The temperature range goes to temperature as low as $T = 0.3$. with the present group size, smaller temperature is not possible. For most simulations, $5000 \sim 8000$ trajectories were obtained, with the first few hundreds removed for thermalization purpose. We did simulation with 3 different lattice size, ($N_t = 8$, $N_x = 8$), ($N_t = 8$, $N_x = 16$), ($N_t = 8$, $N_x = 32$). At low temperature (under $T = 1$), we observed a change of phase and a flat direction problem in the smallest lattice size. Therefore this parameter set is only used at high temperature. In all case, the statistical error is obtained with jackknife analysis.

Figure 19 and 20 show the normalized energy minus pressure as a function of the dimensionless temperature. Figure 19 shows the results at high temperature. The dependence on the space volume $L = aN_x$ is different in the low and high temperature regime resulting in the observed spreading of the data at high temperature. The dashed lines correspond to the prediction from the high temperature expansion.

Figure 20 focuses on the results at low temperature. The dotted line is the theoretical prediction on the gravity side at the leading order. The red and green points correspond to a lattice size of $N_t = 8$, $N_x = 16$ and $N_t = 8$, $N_x = 32$ respectively. The agreement between $T = 0.300$ and $T = 0.4$ is quite good. At higher temperature the contribution of the scale of the string length (α' correction) is important.

In two dimensions we can do the simulation at temperature low enough to observe the leading term on the gravity side. In one dimension, the lattice simulations which is not restrictively slow[16] were only possible down to $T = 0.375$. At this present point in time, we do not know the power of the next to leading order contribution on the gravity side for D1-branes, therefore the few points at low temperature really help to observe the duality quantitatively.

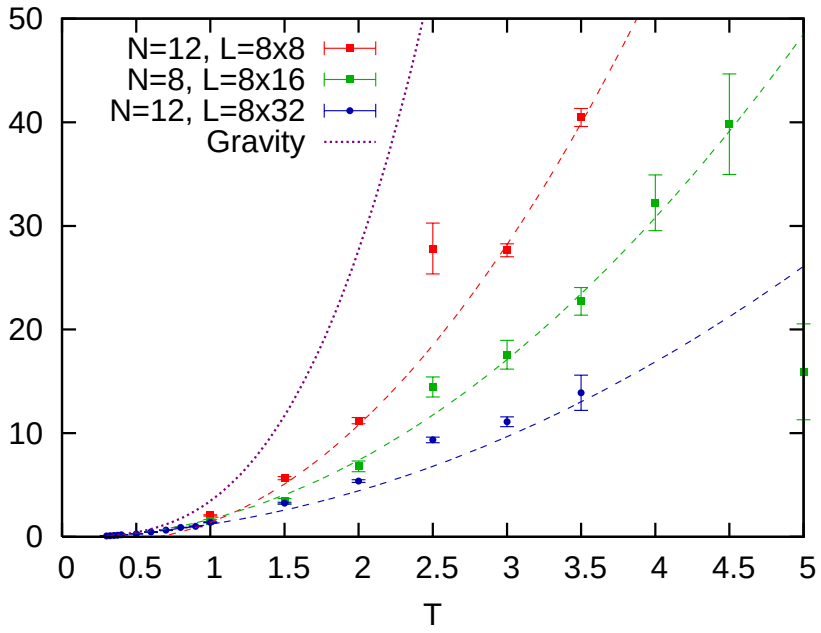

Figure 19: Normalized "energy" $(E - PL)/(N^2 L)$. The line named gravity indicate the expected curve obtained from black p-brane model. The data named Ib correspond to $N = 8$, $N_t = 8$, $N_x = 16$, IIa correspond to $N = 12$, $N_t = 8$, $N_x = 8$ and IIc $N = 12$, $N_t = 8$, $N_x = 32$.

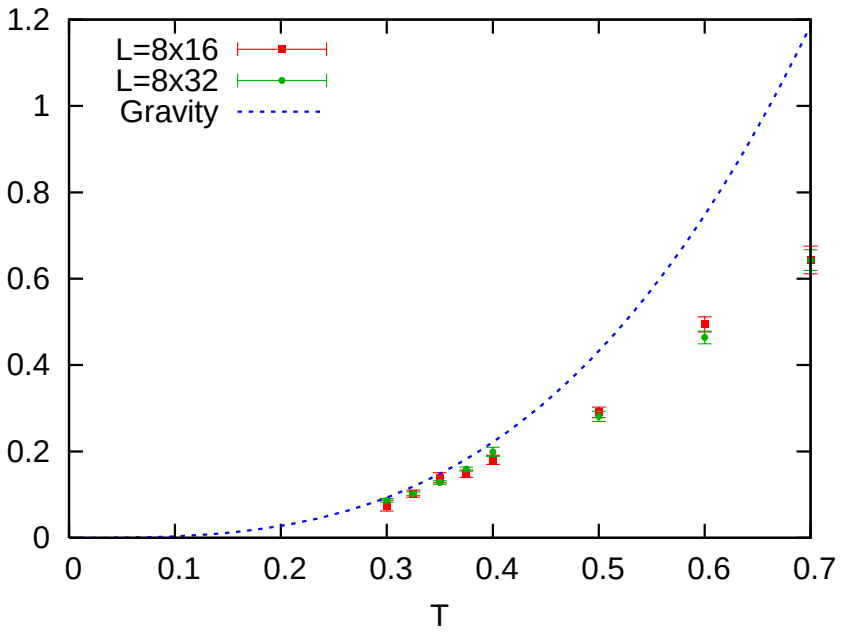

Figure 20: $(E - PL)/(N^2 L)$ at low temperature. The line named gravity indicate the expected curve obtained from black p-brane model: $3.46T^3$. The group size is fixed at $N = 12$.

5 Summary

After confirming the validity of Sugino's lattice formulation, we compared the thermodynamics of $D = 2$ $\mathcal{N} = (8, 8)$ SYM model with those of a D1-brane and found good agreement. From our tests and simulations we found that Sugino's lattice formulation work as expected with the lattice artifact disappearing in the continuous limit. In two dimensions, the flat directions can be suppressed by increasing the space volume, allowing simulations to reach a lower temperature with a smaller gauge group than in one dimension. From the estimation of the supersymmetric Ward-Takahashi identities we confirmed the full supersymmetry is restored in the continuous limit. Therefore the model reach the correct continuum theory in the continuous limit. The action density $\langle S \rangle$ is proportional to the thermodynamic quantity $E - PV$ in two dimensions. This quantity, being a lot more efficient than the energy to obtain during the simulation, was compared with its dual from the gravity side. We observed a good agreement between the theories.

In this study, we do not have enough data yet to observe the correspondence to the next to leading order, which should be visible between $T = 0.4$ and $T = 0.5$. With our simulation, we did manage to get to temperature low enough to clearly see the agreement to the leading order, which was not possible in one dimension. While our statistical error is still quite high, around 10% under $T = 0.4$ where the theories coincide, the overall result is quite convincing: the duality conjecture is true for D1-brane/2D SYM. Further simulation are in progress in order to lower the statistical error and predict the next to leading order contribution.

A Appendix

A.1 Definition of twisted fields

We use two different notations of the fields in this paper. The action (6) is written in the original variables A_μ, X_i, Ψ_α for $\mu = 0, 1,\ i = 2, \cdots, 9,\ \alpha = 1, \cdots, 16$, while the twisted action (11) is written in the twisted variables, $A_\mu, B_i, C, \phi_\pm$ and $\eta_\pm, \psi_{\pm\mu}, \chi_{\pm i}$ for $\mu = 0, 1, 2, 3$ and $i = 0, 1, 2$. In this appendix, we give the relation between the two notations.

Let us express the action (6) written in A_μ, X_i, Ψ_α as the $Q_\pm$-exact action (11) written in the twisted variables $A_\mu, B_i, C, \phi_\pm$. The gauge fields are unchanged, and the other bosonic twisted fields $A_2, A_3, B_i, C, \phi_\pm$ are given as follows:

$$
\begin{aligned}
&A_\mu = X_\mu, \qquad (\mu = 2, 3),\\
&B_0 = -X_6,\\
&B_1 = X_5,\\
&B_2 = -X_4,\\
&C = 2X_7,\\
&\phi_+ = X_8 - iX_9,\\
&\phi_- = -X_8 - iX_9.
\end{aligned}
\tag{163}
$$

The fermionic twisted variables $\eta_\pm, \psi_{\pm\mu}, \chi_{\pm i}$ and Ψ_α can be related to each other by

$$\begin{pmatrix} \Psi_1 \\ \Psi_2 \\ \Psi_3 \\ \Psi_4 \\ \Psi_5 \\ \Psi_6 \\ \Psi_7 \\ \Psi_8 \\ \Psi_9 \\ \Psi_{10} \\ \Psi_{11} \\ \Psi_{12} \\ \Psi_{13} \\ \Psi_{14} \\ \Psi_{15} \\ \Psi_{16} \end{pmatrix} = \frac{1}{\sqrt{2}} \begin{pmatrix} \psi_{-0} + \frac{i}{2}\eta_+ \\ \psi_{-1} - i\chi_{+2} \\ \psi_{-2} + i\chi_{+1} \\ \psi_{-3} - i\chi_{+0} \\ \psi_{+0} + \frac{i}{2}\eta_- \\ \psi_{+1} + i\chi_{-2} \\ \psi_{+2} - i\chi_{-1} \\ \psi_{+3} + i\chi_{-0} \\ -i(\psi_{-0} - \frac{i}{2}\eta_+) \\ -i(\psi_{-1} + i\chi_{+2}) \\ -i(\psi_{-2} - i\chi_{+1}) \\ -i(\psi_{-3} + i\chi_{+0}) \\ -i(\psi_{+0} - \frac{i}{2}\eta_-) \\ -i(\psi_{+1} - i\chi_{-2}) \\ -i(\psi_{+2} + i\chi_{-1}) \\ -i(\psi_{+3} - i\chi_{-0}) \end{pmatrix}, \tag{164}$$

with the following representation of gamma matrices,

$$\begin{aligned} \gamma_1 &= \sigma_2 \otimes \mathbf{1} \otimes \sigma_3 \otimes \sigma_2, \\ \gamma_2 &= \sigma_2 \otimes \mathbf{1} \otimes \sigma_2 \otimes \mathbf{1}, \\ \gamma_3 &= \sigma_2 \otimes \mathbf{1} \otimes \sigma_1 \otimes \sigma_2, \\ \gamma_4 &= \sigma_3 \otimes \sigma_2 \otimes \mathbf{1} \otimes \sigma_2, \\ \gamma_5 &= \sigma_3 \otimes \sigma_2 \otimes \sigma_2 \otimes \sigma_3, \\ \gamma_6 &= \sigma_3 \otimes \sigma_2 \otimes \sigma_2 \otimes \sigma_1, \\ \gamma_7 &= \sigma_3 \otimes \sigma_1 \otimes \mathbf{1} \otimes \mathbf{1}, \\ \gamma_8 &= \sigma_3 \otimes \sigma_3 \otimes \mathbf{1} \otimes \mathbf{1}, \\ \gamma_9 &= \sigma_1 \otimes \mathbf{1} \otimes \mathbf{1} \otimes \mathbf{1}, \end{aligned} \tag{165}$$

where σ_i are the Pauli matrices. [9]

The two scalar supercharges $Q_\pm$ are defined as

$$Q_+ = \frac{1}{\sqrt{2}}(Q_5 - iQ_{13}), \tag{167}$$

$$Q_- = \frac{1}{\sqrt{2}}(Q_1 - iQ_9). \tag{168}$$

The $Q_\pm$-transformations of the fields come from those of Q_α given in (7), (8) and (9).

[9]The gamma matrices act on the fermions ψ_α as $(\gamma_1)_{\alpha_1\alpha_2}\Psi_{\alpha_2}$ where the spinor index α corresponds to the indices of the Pauli matrices as follows:

$$(\gamma_1)_{\alpha_1\alpha_2} = (\sigma_2)_{i_1 i_2} \otimes \mathbf{1}_{j_1 j_2} \otimes (\sigma_3)_{k_1 k_2} \otimes (\sigma_2)_{l_1 l_2}, \tag{166}$$

with $\alpha = 8(i-1) + 4(j-1) + 2(k-1) + l$.

Using the definitions of the twisted fields above and the $Q_{\pm}$-transformations (16), and adding the Gaussian integrals of the auxiliary fields $\tilde{H}_\mu$ and H_i to the action (6), we can rewrite the action (6) as the $Q_{\pm}$-exact form (11).

A.2 Tabulated constant for the high temperature expansion

In the high temperature expansions, many constants are numerically determined.

The first constants are the summations over the modes

$$\sigma_{1/2} - \sigma = \sum_{\vec{n}} \frac{1}{(2\pi)^2(k(n_t+1/2)^2 + n_x^2/k)} - \sum_{\vec{n}\neq 0} \frac{1}{(2\pi)^2(kn_t^2 + n_x^2/k)}, \tag{169}$$

$$\sigma_d = \sum_{\vec{n}} \frac{(k(n_t+1/2)^2 - n_x^2/k)}{(2\pi)^2(k(n_t+1/2)^2 + n_x^2/k)^2} - \sum_{\vec{n}\neq 0} \frac{(kn_t^2 - n_x^2/k)}{(2\pi)^2(kn_t^2 + n_x^2/k)^2}. \tag{170}$$

$$\tag{171}$$

These factors appear in the next to leading order contribution of many quantities. The summations were numerically done to a precision of at 1 to 10000 (absolute). At the extremum of the k spectrum, $k \ll 1$ and $k \gg 1$, the main contributions were calculated analytically. The results are displayed in the table 4.

The HTE model also require numerical simulation for the boson zero modes, represented by the θ_i in our calculation. The form of the S_0 action do not depend on the number of dimension, therefore the value obtained by Nishimura et al. in the one dimensional case can be used. The relation between their results and our notation is

$$\theta_1 = \langle \frac{1}{N} \mathrm{tr}(\hat{A}_a^2) \rangle_0 = \frac{\chi_1}{D-1}, \tag{172}$$

$$\theta_2 = \langle \mathrm{tr}(\hat{A}_a^2)\mathrm{tr}(\hat{A}_a^2) \rangle_0 = \chi_7, \tag{173}$$

$$\theta_3 = \langle \mathrm{tr}(\hat{A}_a^2)\mathrm{tr}(\hat{A}_b^2) \rangle_0 = \frac{\chi_4}{D-1}, \tag{174}$$

$$\theta_4 = \Big\langle \sum_{a,b} \frac{1}{N} \mathrm{tr}(-[\hat{A}_a, \hat{A}_b]^2) tr(\hat{A}_c^2) \Big\rangle_0 = \frac{\chi_5 + \chi_6}{D-1}, \tag{175}$$

$$\theta_5 = \langle \mathrm{tr}(\hat{A}_a^4) \rangle_0 = \chi_8. \tag{176}$$

D is the total number of boson fields, which is constant in both notation. The θ_6 can be analytically calculated,

$$\theta_6 = \langle -\frac{N}{4} \mathrm{tr}[\hat{A}_a, \hat{A}_b][\hat{A}_a, \hat{A}_b] \rangle_0 = \frac{D}{4}(N^2-1). \tag{177}$$

Table 5 contains the part of the original table which contains the constant that we used in the present study.

k	$\sigma_{1/2} - \sigma$	σ_d
$k \ll 1$	$1/6k$	$-1/6k$
0.3	0.5556(1)	-0.5556(1)
0.5	0.3334(1)	-0.3334(1)
0.6	0.2778(1)	-0.2780(1)
0.7	0.2381(1)	-0.2388(1)
0.8	0.2082(1)	-0.2103(1)
0.9	0.1847(1)	-0.1893(1)
1.0	0.1655(1)	-0.1742(1)
1.1	0.1495(1)	-0.1636(1)
1.2	0.1356(1)	-0.1567(1)
1.3	0.1232(1)	-0.1529(1)
1.4	0.1119(1)	-0.1515(1)
1.5	0.1014(1)	-0.1522(1)
1.6	0.0915(1)	-0.1545(1)
1.7	0.0821(1)	-0.1580(1)
1.8	0.0729(1)	-0.1626(1)
1.9	0.0640(1)	-0.1681(1)
2.0	0.0552(1)	-0.1742(1)
2.1	0.0466(1)	-0.1807(1)
2.2	0.0380(1)	-0.1877(1)
2.3	0.0295(1)	-0.1950(1)
2.4	0.0210(1)	-0.2026(1)
2.5	0.0126(1)	-0.2103(1)
2.6	0.0042(1)	-0.2181(1)
2.7	-0.0042(1)	-0.2261(1)
2.8	-0.0126(1)	-0.2342(1)
2.9	-0.0209(1)	-0.2423(1)
3.0	-0.0293(1)	-0.2505(1)
3.1	-0.0376(1)	-0.2587(1)
3.2	-0.0460(1)	-0.2669(1)
3.3	-0.0543(1)	-0.2752(1)
3.4	-0.0626(1)	-0.2835(1)
3.5	-0.0710(1)	-0.2918(1)
3.6	-0.0793(1)	-0.3001(1)
3.7	-0.0877(1)	-0.3084(1)
3.8	-0.0960(1)	-0.3167(1)
3.9	-0.1043(1)	-0.3250(1)
4.0	-0.1127(1)	-0.3334(1)
4.2	-0.1293(1)	-0.3500(1)
4.4	-0.1460(1)	-0.3667(1)
4.6	-0.1627(1)	-0.3833(1)
4.8	-0.1793(1)	-0.4000(1)
5.0	-0.1960(1)	-0.4167(1)
$k \gg 1$	$0.2207(1) - k/12$	$-k/12$

Table 4: Tabulated value of the momentum summation contribution for the HTE.

N	χ_1	χ_3	χ_4	χ_5	χ_6	χ_7	χ_8
4	2.191(1)	0.769(5)	-0.0925(5)	3.99(1)	-0.558(2)	0.1681(6)	0.1199(1)
8	2.2700(2)	0.746(1)	-0.0861(3)	4.34(1)	-0.510(1)	0.1595(2)	0.12894(3)
10	2.2810(5)	0.766(3)	-0.0859(6)	4.44(2)	-0.506(3)	0.1615(5)	0.13045(7)
12	2.2854(3)	0.751(4)	-0.0863(6)	4.44(2)	-0.510(1)	0.1602(2)	0.13114(3)
16	2.2901(1)	0.746(2)	-0.0886(5)	4.43(1)	-0.525(3)	0.1617(2)	0.13163(2)
20	2.2932(3)	0.734(3)	-0.0912(9)	4.40(2)	-0.55(1)	0.1631(6)	0.13204(3)
32	2.29566(7)	0.730(6)	-0.082(1)	4.38(2)	-0.59(1)	0.1399(1)	0.13234(1)
∞	2.2975(1)	0.719(6)	-0.082(6)	4.36(2)	-0.61(2)	0.14(2)	0.13257(5)

Table 5: The values of χ_i as obtained by Nishimura et al. in [41] obtained by Monte Carlo simulation. Only the value corresponding to the 16 supersymmetry case are included, for the full table see the original publication.

References

[1] S. Dasari, A. Kumar Biswas, *An Economic analogy to Electrodynamics,* [arXiv:1001.1847v5]

[2] J. M. Maldacena, *The Large N limit of superconformal field theories and supergravity,* Int. J. Theor. Phys. **38** (1999) 1113 [Adv. Theor. Math. Phys. **2** (1998) 231] [hep-th/9711200].

[3] O. Aharony, O. Bergman, D. L. Jafferis and J. Maldacena, *N=6 superconformal Chern-Simons-matter theories, M2-branes and their gravity duals,* JHEP **0810** (2008) 091 [arXiv:0806.1218 [hep-th]].

[4] N. Itzhaki, J. M. Maldacena, J. Sonnenschein and S. Yankielowicz, *Supergravity and the large N limit of theories with sixteen supercharges,* Phys. Rev. D **58** (1998) 046004 [hep-th/9802042].

[5] J. Dai, R. G. Leigh and J. Polchinski, *New Connections Between String Theories,* Mod. Phys. Lett. A **4** (1989) 2073.

[6] J. Polchinski, *Dirichlet Branes and Ramond-Ramond charges,* Phys. Rev. Lett. **75** (1995) 4724 [hep-th/9510017].

[7] G. T. Horowitz and A. Strominger, *Black strings and P-branes,* Nucl. Phys. B **360** (1991) 197.

[8] A. Strominger and C. Vafa, *Microscopic origin of the Bekenstein-Hawking entropy,* Phys. Lett. B **379** (1996) 99 [hep-th/9601029].

[9] I. R. Klebanov, *TASI lectures: Introduction to the AdS/CFT correspondence,* hep-th/0009139. J. M. Maldacena, *TASI 2003 lectures on AdS/CFT,* hep-th/0309246. J. Polchinski, *Introduction to Gauge/Gravity Duality,* arXiv:1010.6134 [hep-th]. T. Gherghetta, *TASI Lectures on a Holographic View of Beyond the Standard Model Physics,* arXiv:1008.2570 [hep-ph].

[10] E. Witten, *Anti-de Sitter space and holography* Adv. Theor. Math. Phys. **2** (1998) 253 [hep-th/9802150].

[11] S. S. Gubser, I. R. Klebanov and A. M. Polyakov, *Gauge theory correlators from noncritical string theory,* Phys. Lett. B **428** (1998) 105 [hep-th/9802109].

[12] T. Sakai and S. Sugimoto, *Low energy hadron physics in holographic QCD,* Prog. Theor. Phys. **113** (2005) 843 [hep-th/0412141].

[13] C. P. Herzog, *Lectures on Holographic Superfluidity and Superconductivity,* J. Phys. A **42** (2009) 343001 [arXiv:0904.1975 [hep-th]].

[14] S. W. Hawking, *Breakdown of Predictability in Gravitational Collapse,* Phys. Rev. D **14** (1976) 2460. *The Unpredictability of Quantum Gravity,* Commun. Math. Phys. **87** (1982) 395.

[15] K. N. Anagnostopoulos, M. Hanada, J. Nishimura and S. Takeuchi, *Monte Carlo studies of supersymmetric matrix quantum mechanics with sixteen supercharges at finite temperature,* Phys. Rev. Lett. **100** (2008) 021601 [arXiv:0707.4454 [hep-th]]. M. Hanada, A. Miwa, J. Nishimura and S. Takeuchi, *Schwarzschild radius from Monte Carlo calculation of the Wilson loop in supersymmetric matrix quantum mechanics,* Phys. Rev. Lett. **102** (2009) 181602 [arXiv:0811.2081 [hep-th]]. M. Hanada, Y. Hyakutake, J. Nishimura and S. Takeuchi, *Higher derivative corrections to black hole thermodynamics from supersymmetric matrix quantum mechanics,* Phys. Rev. Lett. **102** (2009) 191602 [arXiv:0811.3102 [hep-th]]. M. Hanada, J. Nishimura, Y. Sekino and T. Yoneya, *Monte Carlo studies of Matrix theory correlation functions,* Phys. Rev. Lett. **104** (2010) 151601 [arXiv:0911.1623 [hep-th]]. *Direct test of the gauge-gravity correspondence for Matrix theory correlation functions,* JHEP **1112** (2011) 020 [arXiv:1108.5153 [hep-th]]. M. Hanada, Y. Hyakutake, G. Ishiki and J. Nishimura, *Holographic description of quantum black hole on a computer,* Science **344** (2014) 882 [arXiv:1311.5607 [hep-th]].

[16] D. Kadoh and S. Kamata, *Gauge/gravity duality and lattice simulations of one dimensional SYM with sixteen supercharges,* arXiv:1503.08499 [hep-lat].

[17] S. Catterall, A. Joseph and T. Wiseman, *Gauge theory duals of black hole - black string transitions of gravitational theories on a circle,* J. Phys. Conf. Ser. **462** (2013) 1, 012022 [arXiv:1009.0529 [hep-th]]. *Thermal phases of D1-branes on a circle from lattice super Yang-Mills,* JHEP **1012** (2010) 022 [arXiv:1008.4964 [hep-th]]. S. Catterall and T. Wiseman, *Towards lattice simulation of the gauge theory duals to black holes and hot strings,* JHEP **0712** (2007) 104 [arXiv:0706.3518 [hep-lat]]. *Black hole thermodynamics from simulations of lattice Yang-Mills theory,* Phys. Rev. D **78** (2008) 041502 [arXiv:0803.4273 [hep-th]]. *Extracting black hole physics from the lattice,* JHEP **1004** (2010) 077 [arXiv:0909.4947 [hep-th]].

[18] Kenneth G. Wilson, *Confinement of quarks,* Physical Review D, vol. 10, Issue 8, pp. 2445-2459

[19] Nielsen, H.B.; Ninomiya, M. (1981), *A no-go theorem for regularizing chiral fermions*, Phys. Lett. B105: 219

[20] M. Kato, M. Sakamoto and H. So, *No-Go Theorem of Leibniz Rule and Supersymmetry on the Lattice*, PoS LATTICE **2008** (2008) 233 [arXiv:0810.2360 [hep-lat]].

[21] D. B. Kaplan, E. Katz and M. Unsal, *Supersymmetry on a spatial lattice,* JHEP **0305** (2003) 037 [hep-lat/0206019]. A. G. Cohen, D. B. Kaplan, E. Katz and M. Unsal, *Supersymmetry on a Euclidean space-time lattice. 1. A Target theory with four supercharges,* JHEP **0308** (2003) 024 [hep-lat/0302017]. *Supersymmetry on a Euclidean space-time lattice. 2. Target theories with eight supercharges,* JHEP **0312** (2003) 031 [hep-lat/0307012]. D. B. Kaplan and M. Unsal, *A Euclidean lattice construction of supersymmetric Yang-Mills theories with sixteen supercharges,* JHEP **0509** (2005) 042 [hep-lat/0503039]. M. G. Endres and D. B. Kaplan, *Lattice formulation of (2,2) supersymmetric gauge theories with matter fields,* JHEP **0610** (2006) 076 [hep-lat/0604012].

[22] F. Sugino, *A Lattice formulation of superYang-Mills theories with exact supersymmetry,* JHEP **0401** (2004) 015 [hep-lat/0311021].

[23] F. Sugino, *SuperYang-Mills theories on the two-dimensional lattice with exact supersymmetry,* JHEP **0403** (2004) 067 [hep-lat/0401017].

[24] F. Sugino, *Various super Yang-Mills theories with exact supersymmetry on the lattice,* JHEP **0501** (2005) 016 [hep-lat/0410035].

[25] F. Sugino, *Two-dimensional compact N=(2,2) lattice super Yang-Mills theory with exact supersymmetry,* Phys. Lett. B **635** (2006) 218 [hep-lat/0601024]. *Lattice Formulation of Two-Dimensional N=(2,2) SQCD with Exact Supersymmetry,* Nucl. Phys. B **808** (2009) 292 [arXiv:0807.2683 [hep-lat]]. Y. Kikukawa and F. Sugino, *Ginsparg-Wilson Formulation of 2D N = (2,2) SQCD with Exact Lattice Supersymmetry,* Nucl. Phys. B **819** (2009) 76 [arXiv:0811.0916 [hep-lat]]. D. Kadoh, F. Sugino and H. Suzuki, *Lattice formulation of 2D N = (2,2) SQCD based on the B model twist,* Nucl. Phys. B **820** (2009) 99 [arXiv:0903.5398 [hep-lat]].

[26] S. Matsuura and F. Sugino, *Lattice formulation for 2d = (2, 2), (4, 4) super Yang-Mills theories without admissibility conditions,* JHEP **1404** (2014) 088 [arXiv:1402.0952 [hep-lat]].

[27] S. Catterall, *A Geometrical approach to N=2 super Yang-Mills theory on the two dimensional lattice,* JHEP **0411** (2004) 006 [hep-lat/0410052]. *Lattice formulation of N=4 super Yang-Mills theory,* JHEP **0506** (2005) 027 [hep-lat/0503036].

[28] A. D'Adda, I. Kanamori, N. Kawamoto and K. Nagata, *Exact extended supersymmetry on a lattice: Twisted N=2 super Yang-Mills in two dimensions,* Phys. Lett. B **633** (2006) 645 [hep-lat/0507029]. *Exact Extended Supersymmetry on a Lattice: Twisted N=4 Super Yang-Mills in Three Dimensions,* Nucl. Phys. B **798** (2008) 168 [arXiv:0707.3533 [hep-lat]].

[29] S. Matsuura, *Two-dimensional N=(2,2) Supersymmetric Lattice Gauge Theory with Matter Fields in the Fundamental Representation,* JHEP **0807** (2008) 127 [arXiv:0805.4491 [hep-th]].

[30] A. Joseph, *Lattice formulation of three-dimensional $\mathcal{N} = 4$ gauge theory with fundamental matter fields,* JHEP **1309** (2013) 046 [arXiv:1307.3281 [hep-lat]]. *Supersymmetric quiver gauge theories on the lattice,* JHEP **1401** (2014) 093 [arXiv:1311.5111 [hep-lat], arXiv:1311.5111]. *Two-dimensional $\mathcal{N}$ = (2, 2) lattice gauge theories with matter in higher representations,* JHEP **1407** (2014) 067 [arXiv:1403.4390 [hep-lat]].

[31] I. Montvay, *Supersymmetric Yang-Mills theory on the lattice,* Int. J. Mod. Phys. A **17** (2002) 2377 [hep-lat/0112007].

[32] J. P. Costella, *A New proposal for the fermion doubling problem,* hep-lat/0207008. J. P. Costella, *A New proposal for the fermion doubling problem. 2. Improving the operators for finite lattices,* hep-lat/0207015.

[33] A. D'Adda, I. Kanamori, N. Kawamoto and J. Saito, *Species Doublers as Super Multiplets in Lattice Supersymmetry: Chiral Conditions of Wess-Zumino Model for D=N=2* JHEP **1203** (2012) 043 [arXiv:1107.1629 [hep-lat]]. A. D'Adda, A. Feo, I. Kanamori, N. Kawamoto and J. Saito, *Species Doublers as Super Multiplets in Lattice Supersymmetry: Exact Supersymmetry with Interactions for D=1 N=2,* JHEP **1009** (2010) 059 [arXiv:1006.2046 [hep-lat]].

[34] R. Dijkgraaf and G. W. Moore, *Balanced topological field theories,* Commun. Math. Phys. **185** (1997) 411 [hep-th/9608169]. C. Vafa and E. Witten, *A Strong coupling test of S duality,* Nucl. Phys. B **431** (1994) 3 [hep-th/9408074]. J. M. F. Labastida and C. Lozano, *Mathai-Quillen formulation of twisted N=4 supersymmetric gauge theories in four-dimensions,* Nucl. Phys. B **502** (1997) 741 [hep-th/9702106]. M. Blau and G. Thompson, *Aspects of N(T) ¿= two topological gauge theories and D-branes,* Nucl. Phys. B **492** (1997) 545 [hep-th/9612143].

[35] M. Hanada, S. Matsuura and F. Sugino, *Two-dimensional lattice for four-dimensional N=4 supersymmetric Yang-Mills* Prog. Theor. Phys. **126** (2011) 597 [arXiv:1004.5513 [hep-lat]].

[36] A. Frommer, B. Nockel, S. Gusken, T. Lippert and K. Schilling, *Many masses on one stroke: Economic computation of quark propagators,* Int. J. Mod. Phys. C **6** (1995) 627 [hep-lat/9504020]. B. Jegerlehner, *Krylov space solvers for shifted linear systems.* hep-lat/9612014.

[37] M. A. Clark and A. D. Kennedy, http://www.ph.ed.ac.uk/˜mike/remez, 2005.

[38] Anderson, E. et al., *LAPACK Users' Guide, third edition (1999),* Society for Industrial and Applied Mathematics.

[39] I. Kanamori and H. Suzuki, *Restoration of supersymmetry on the lattice: Two-dimensional N = (2,2) supersymmetric Yang-Mills theory,* Nucl. Phys. B **811** (2009) 420 [arXiv:0809.2856 [hep-lat]].

[40] I. R. Klebanov and A. A. Tseytlin, *Entropy of near extremal black p-branes,* Nucl. Phys. B **475** (1996) 164 [hep-th/9604089].

[41] N. Kawahara, J. Nishimura and S. Takeuchi, *High temperature expansion in supersymmetric matrix quantum mechanics*, JHEP **0712** (2007) 103 [arXiv:0710.2188 [hep-th]].

[42] V. Pestun, *Localization of gauge theory on a four-sphere and supersymmetric Wilson loops,* Commun. Math. Phys. **313** (2012) 71 [arXiv:0712.2824 [hep-th]].

[43] J. K. Erickson, G. W. Semenoff and K. Zarembo, *Wilson loops in N=4 supersymmetric Yang-Mills theory,* Nucl. Phys. B **582** (2000) 155 [hep-th/0003055]. N. Drukker, *1/4 BPS circular loops, unstable world-sheet instantons and the matrix model,* JHEP **0609** (2006) 004 [hep-th/0605151].

[44] M. A. Clark, A. D. Kennedy and Z. Sroczynski, *Exact 2+1 flavour RHMC simulations,* Nucl. Phys. Proc. Suppl. **140** (2005) 835 [hep-lat/0409133].